CELLULOSE NANO FIBERS INFUSED POLYLACTIC ACID USING THE PROCESS OF TWIN SCREW MELT EXTRUSION FOR 3D PRINTING APPLICATIONS

by

Siddharth Bhaganagar

A Thesis

Submitted to the Faculty of Purdue University

In Partial Fulfillment of the Requirements for the degree of

Master of Science in Engineering

Department of Motorsport Engineering at IUPUI

Indianapolis, Indiana

May 2023

THE PURDUE UNIVERSITY GRADUATE SCHOOL
STATEMENT OF COMMITTEE APPROVAL

Dr. Hamid Dalir, Co-Chair

Department of Motorsport Engineering

Dr. Mangilal Agarwal, Co-Chair

Department of Mechanical Engineering

Dr. Jing Zhang

Department of Mechanical Engineering

Approved by:

Dr. Hamid Dalir

Dedicated to my family and friends for their endless love, support and encouragement.

ACKNOWLEDGMENTS

I'd like to express my gratitude to Dr. Hamid Dalir, my esteemed advisor, for all the guidance, support, and instruction he provided me throughout my master's degree. I would like to thank Dr. Zhang for providing me with the resources to conduct my experiments.

In addition, I'd like to thank Dr. Agarwal, whose invaluable feedback and encouragement greatly influenced how I conducted my experiments and interpreted my findings. Drs. Dalir, Agarwal, and Zhang have been incredible mentors, and I'm also grateful to them. Friends, lab mates, colleagues, and research team in the Advanced Composite Structures Engineering Laboratory and Integrated Nano-systems Development Institute are all appreciated for the fun times we had working and socializing together. I'd also like to thank everyone who has been there for me emotionally and intellectually as I've worked on my coursework.

Lastly, I would be remiss in not mentioning my family, especially my parents. Their belief in me has kept my spirits and motivation high during this process.

TABLE OF CONTENTS

LIST OF TABLES

LIST OF FIGURES

ABSTRACT

In this thesis, cellulose nanofiber (CNF) reinforced polylactic acid (PLA) filaments were produced for 3D printing applications using melt extrusion. The use of CNF reinforcement has the potential to improve the mechanical properties of PLA, making it a more suitable material for various 3D printing applications. To produce the nanocomposites, a master batch with a high concentration of CNFs was premixed with PLA, and then diluted to final concentrations of 1, 3, and 5 wt% during the extrusion process. The dilution was carried out to assess the effects of varying CNF concentrations on the morphology and mechanical properties of the composites. The results showed that the addition of 3 wt.% CNF significantly enhanced the mechanical properties of the PLA composites. Specifically, the tensile strength increased by 77.7%, the compressive strength increased by 62.7%, and the flexural strength increased by 60.2%. These findings demonstrate that the melt extrusion of CNF reinforced PLA filaments is a viable approach for producing nanocomposites with improved mechanical properties for 3D printing applications. In conclusion, the study highlights the potential of CNF reinforcement in improving the mechanical properties of PLA for 3D printing applications. The results can provide valuable information for researchers and industries in the field of 3D printing and materials science, as well as support the development of more advanced and sustainable 3D printing materials.

1. INTRODUCTION

By shaping and manufacturing complex structures cost-effectively, 3D printing is transforming the industrial landscape. In recent years, numerous materials have been developed for 3D printing applications, including polylactic acid (PLA) melt extruded with cellulose nanofibrils (CNF). CNF-infused PLA melt extrusion provides a number of advantages over traditional methods of 3D printing, such as increased strength and superior dimensional accuracy. Despite its potential as an alternative 3D printing material, there have been limited studies exploring the use of PLA melt extruded with CNF for 3D printing applications. In order to address this, this paper investigates the potential of PLA melt extruded with CNF for 3D printing applications from a material and performance perspective. A comprehensive review of recent research and development in this area is presented in this study along with insights into the opportunities and challenges associated with this innovative application.

1.1 3D Printing

The 3D printing process may produce physical objects by building them up from computer models in a variety of thin layers of a material. It converts a computer item's CAD model into its physical shape by adding layers of materials.

A multitude of techniques can be used to 3D print an item. We shall go into further depth later on in the chapter. Two significant developments made possible by 3D printing are the capacity to alter objects in their digital form and the creation of new forms by the addition of material.

Technology has most certainly recently made a substantial influence more than any previous period in history. The development of the lighting, the steam engine, or more recently, the vehicle and the airplane, not to mention the continuous growth of the internet, should all be taken into consideration. Even while these technologies have greatly enriched our lives and opened up new possibilities, it sometimes takes years or even decades for their disruptive potential to be completely realized.

One of these technologies is commonly thought to have a lot of potential to emerge from additive manufacturing, often known as 3D printing. 3D printing has now been extensively covered in print, internet, and televised media. What precisely is 3D printing, which some believe will transform design, terminate traditional manufacturing as we know it, and have an influence on geopolitics, economics, society, demography, the environment, and security in our day-to-day lives?

The utilization of an additive manufacturing process is the key distinguishing factor of 3D printing. This is important because 3D printing is a fundamentally new manufacturing technique that makes products additively in layers at a sub-mm scale using cutting-edge technology. The primary distinctions between this and other current conventional production techniques.

Many problems plague traditional manufacturing. It has always placed a high priority on manual work and the made-by-hand ethic, which originates with the French term for production. Nonetheless, the manufacturing sector has developed, and automated processes such as machining, casting, forming, and molding are all (relatively) contemporary, sophisticated processes that need equipment, technology, and robots.

All of these methods, however, need material to be removed from a larger block in order to create the completed product or a tool for casting or molding processes, which places a considerable limitation on the production process as a whole.

For many applications, traditional design and production processes impose a number of intolerably onerous restrictions, such as the pricy tooling mentioned above, fixtures, and the necessity of assembly for intricate pieces. Moreover, waste generated by subtractive manufacturing processes like machining might amount to 90% of the original material block. On the other hand, depending on the technology used, 3D printing is a method for directly creating products by stacking material. For those who are still trying to grasp the concept, 3D printing may be simplified to be like the automated process of building anything out of Lego parts (and there are many).

3D printing is an enabling technology that fosters and drives innovation while minimizing prohibitive costs and lead times. It offers unmatched design flexibility and toollessness. To avoid

the requirement for assembly, components can be created specifically with complicated features and advanced geometry at no extra cost. Due to the usage of up to 90% standard materials, 3D printing is also proven to be an energy-efficient method that might have a positive influence on the environment throughout the course of the product's life due to its lighter and stronger construction.

Nowadays, the cost of the technology has decreased, and 3D printing is now more than merely an industrial research and manufacturing process. Smaller (less capable) 3D printers, once the domain of huge, multinational corporations, may now be acquired for approximately $1000 due to the scale and economics of owning one.

The technology is now available to a far wider audience, and as a result, more systems, materials, applications, services, and ancillaries are being developed as the exponential adoption rate picks up speed on all fronts.

Background

The first antecedents of 3D printing, known as rapid prototyping (RP) technology, first came into the public eye in the late 1980s. This is because the methods were initially intended to be a speedier and more practical means of producing prototypes for product development inside industry. A fascinating side fact is that the first patent application for RP technology was made in May 1980 by Dr. Kodama of Japan. Unfortunately for Dr. Kodama, despite the fact that he was a patent attorney, the entire invention specification was not later filed before the application's one-year deadline. Yet, the first patent for a stereolithography equipment was issued in 1986, which is when 3D printing was first invented (SLA). The proprietor of this innovation is Charles (Chuck) Hull, who built his SLA machine in 1983. In the future, Hull co-founded 3D Systems Corporation, one of the biggest and most prosperous companies in the 3D printing market right now. After rigorous testing, the first SLA-1 RP system from 3D Systems was delivered in 1988. The SLA-1 was the company's first commercially available RP system. While SLA might claim to have been the first RP technology to cross the finish line, it wasn't the only one being created at the time. The Selective Laser Sintering (SLS) RP procedure was actually the subject of a patent application in the US submitted by Carl Deckard in 1987 when he was employed at the University of Texas. This

invention was issued in 1989, and SLS subsequently acquired a license from DTM Inc. that 3D Systems later acquired.

Another 1989 patent application on fused deposition modeling (FDM) was filed by co-founder of Stratasys Inc. Scott Crump. The procedure used by many of the entry-level machines that are currently in use that are based on the open source RepRap model is called FDM, and it is a proprietary technology that the firm still owns. Stratasys received the FDM patent in 1992. Hans Langer's EOS GmbH was also introduced to Europe in 1989. EOS' R&D concentration was mostly on the laser sintering (LS) process, which has advanced, after a brief flirtation with SL techniques. The EOS systems are already well-known across the world for their high-quality output for commercial 3D printing applications and industrial prototypes. In 1990, EOS sold its first "Stereos" system. A pilot experiment with an Electrolux Finland subsidiary that was later bought by EOS led to the development of the company's direct metal laser sintering (DMLS) procedure.

Other 3D printing technologies and processes, such as the "three dimensional printing" (3DP) created by Emanuel Sachs et al. and initially patented by William Masters, the laminated object manufacturing (LOM), the solid ground curing (SGC), and the ballistic particle manufacturing (BPM) by Michael Feygin, were also developing at this time. Just three of the original companies are still in business today: 3D Systems, EOS, and Stratasys. The RP sector witnessed a rise in competitiveness in the early 1990s.

The 1990s and the beginning of the 2000s saw the introduction of several new technologies, however they were still mostly procedures for prototyping applications. In-depth tooling, casting, and direct production applications were the focus of R&D by the most advanced technology vendors. As a result, the words "Rapid Tooling," "Rapid Casting," and "Rapid Manufacturing" were coined.

In the context of business activities, Sanders Prototype (later Solidscape) and ZCorporation were founded in 1996, Arcam in 1997, Objet Geometries in 1998, MCP Technologies (an established vacuum casting OEM) introduced the SLM technology in 2000, EnvisionTec in 2002, ExOne in 2005 as a switch from the Extrude Hone Corporation, and Sciaky Inc., which was pioneering it in

2006, was developing its own additive process based on its exclusive electron beam welding All of these businesses contributed to the growth of Western businesses operating abroad.Due to the expansion of manufacturing applications, the vocabulary had evolved, and the term "additive manufacturing" had come to represent all of the processes (AM). Significantly, the Eastern Hemisphere was seeing significant growth on par with that in the West. Although they had considerable local success at the time and were significant in and of themselves, these innovations had little impact on the global market.

Around the middle of the 2000s, the business started to show major signs of diversification, concentrating on two areas in particular that are now considerably more distinct. The most advanced, most expensive 3D printing technologies existed in the past, and they were made for making intricate, valuable things that required substantial engineering. Even while this is still ongoing and growing, industrial applications in the aerospace, automotive, medical, and fine jewelry sectors are just now beginning to demonstrate the benefits. This is due to the fact that years of R&D and certification are starting to profit.

Several items continue to be secret or protected by non-disclosure agreements (NDA). On the other end of the spectrum, various manufacturers of 3D printing technologies were developing and improving what were at the time referred to as "concept modellers." With an emphasis on accelerating concept generation and useful prototype, these 3D printers were developed primarily as user- and office-friendly, cost-effective solutions. the ancestor of contemporary desktop computers. Nonetheless, the main focus of each of these regimes was remained industry.

The lower end of the market for 3D printers, which are today regarded as being in the mid-range, saw a price war as well as slight improvements in printing accuracy, speed, and materials.

In 2007, 3D Systems released its first sub-$10,000 system, however it fell short of expectations. In addition to the technology itself, a number of market considerations were also an influence. At the time, finding a 3D printer for less than $5000 was the holy grail since it would make the technology accessible to a far bigger audience.

The most anticipated event of that year was the launch of the much anticipated Desktop Factory, which many said would bring that holy grail into being. The organization had difficulties leading up to the production, which contributed to its failure. Cathy Lewis, the company's creator, and the IP were all acquired by 3D Systems in 2008. After then, Desktop Factory has almost completely vanished. Though few were aware of it at the time, the RepRap mania that started in 2007 really signaled the beginning of the end for 3D printing technology that was accessible to the general public.

Dr. Bowyer came up with the concept for the RepRap, an open-source, self-replicating 3D printer, in 2004. His Bath team, especially Vik Oliver and Rhys Jones, put in a lot of effort over the next years to develop the concept into working prototypes of a 3D printer that makes use of the deposition process. The emergence of this open source 3D printing movement began to show its first hints in 2007.

It took until January 2009 for the first commercially produced 3D printer based on the RepRap concept to become available for purchase. From BfB RapMan, this was a 3D printer. In April of the same year, Makerbot Industries, whose founders had played a vital role in the creation of RepRap before abandoning the Open Source philosophy after substantial investment, lagged behind.

Since 2009, there have been and continue to be several deposition printers with minor unique selling propositions (USPs). The amazing contradiction in this situation is that, despite the fact that the RepRap boom has created a brand-new market for entry-level, commercial 3D printers, the community's mindset is totally focused on Open Source advancements for 3D printing and against commercialization.

In 2012, new 3D printing methods first became commercially available at the entry level. After the B9Creator (using DLP technology) in June, the Form 1 (using stereolithography) came in December. Both of the initiatives, which were both funded through the crowdsourcing website Kickstarter, were huge successes.

Due to the market split, important developments in industrial capabilities and applications, a sharp rise in awareness and adoption across a developing maker movement, and these circumstances, 2012 was also the year when many different mainstream media outlets started to cover the technology. 2013 saw a lot of expansion and consolidation. One of the most notable events was when Stratasys bought Makerbot.

There is no denying the impact that 3D printing is having on industry, as well as the great promise that technology has for consumers in the future. Others have called it the second, third, and occasionally even fourth Industrial Revolution. We're still figuring out how that potential will manifest itself.

Working

Each 3D printing process starts with the creation of a 3D digital model, which may be done with a variety of 3D software tools, including 3D CAD (which is used in industry) or by scanning a real thing with a 3D scanner. After being "sliced" into layers, the design is then converted into a format that the 3D printer can understand. Afterwards, in line with the procedure and design, the 3D-printed material is stacked. As was previously stated, there are several distinct types of 3D printing technologies, and each one employs a different technique to process a different type of material to create the final product. Functional plastics, metals, ceramics, and sand are used in industrial prototype and production applications regularly nowadays. Moreover, studies on 3D printing biomaterials and other food types are being conducted. The bottom end of the market, however, is often where materials are much more restricted. Plastic is the sole substance that is now widely utilized; it is frequently composed of ABS or PLA, however Nylon is one of a growing number of alternatives. Moreover, there are more and more entry-level devices that have been tuned to handle substances like sugar and chocolate.

The many types of 3D printers employ different technologies that handle different materials in different ways. Understanding that there is no "one size fits all" solution when it comes to the materials and applications for 3D printing is essential. This is one of the technology's most fundamental limitations. To provide an example, some 3D printers use powdered materials (such metal, nylon, plastic, and ceramic) and a light or heat source to sinter, melt, or fuse layers of the

powder together into the desired shape. Others treat the components of polymer resin using a light or laser before layering the resin to solidify it. A different 3D printing method is called jetting, which is similar to 2D inkjet printing but employs superior materials and a binder to keep the layers in place.

The majority of entry-level 3D printers employ deposition, which is possibly the most used and most recognized technique. With this technique, heated plastic filaments—usually PLA or ABS—are extruded via an extruder to create layers and the desired form.

Due to the fact that components may be printed directly, intricate and highly detailed goods can be made without the need for assembly because functionality is frequently included right into the design.

Another essential issue to stress is the fact that none of the 3D printing processes are now offered as plug-and-play options. Before pressing the print button, there are a number of steps that must be taken, and there are even more once the document has been taken out of the printer. File preparation and conversion may be time-consuming and difficult in addition to the difficult realities of designing for 3D printing, especially for objects that require intricate supports during manufacturing. Yet, the problem is becoming improved as a result of periodic software updates and upgrades. After being taken out of the printer, numerous components will also need to go through finishing procedures. The obvious one for support-required procedures is support removal, but other examples include sanding, lacquering, painting, or other traditional finishing touches, all of which often need to be done by hand and need ability, as well as time and patience.
Techniques for printing

Stereolithography

Stereolithography (SL), frequently regarded as the first 3D printing technique, was definitely the first to gain widespread commercialization. SL is a laser-based technology that creates exceptionally exact components by curing photopolymer resins in a highly precise manner. The photopolymer resin is housed in a vat that has an internal moving platform, albeit it is difficult to define simply. In accordance with the 3D data (the.stl file) that was sent to the machine, a laser is

directed in the X-Y axes over the resin's surface. As a result, the resin hardens exactly where the laser makes contact with the surface.

When the first layer is finished, a little portion (in the Z axis) of the platform inside the vat is removed, and the laser then draws out the second layer. When everything has developed, the platform may be removed from the vat and moved.

As a result of the type of the SL process, some items, especially those with hangs or cuts, require structures to support them. Removal of this manually is often required.

Cleaning and curing are additional post-processing steps for many SL-printed products. Curing involves placing the component in a device like an oven and exposing it to intense light in order to thoroughly harden the resin. Stereolithography, with its exceptional surface polish, is one of the most exact 3D printing techniques, according to the majority of specialists. Limiting factors, however, include the required post-processing steps and the materials' endurance with time, which can become more brittle.

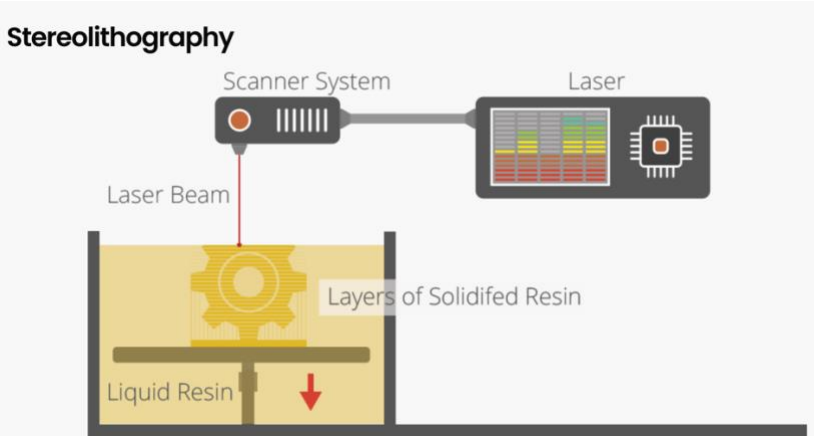

Figure 1. Stereolithography

FDM

Without a doubt, extruding thermoplastic material to make 3D models is the most well-known and widely used 3DP technique. Due to its length, the technique is most frequently referred to as "fused deposition modeling" (FDM), however this is really a trademark registered by Stratasys, the

company that first developed it. Since the early 1990s, industrial-grade 3D printing has been accomplished using Stratasys' FDM technology. However because Stratasys still holds the patents, the plethora of inexpensive 3D printers that have emerged since 2009 primarily employ a related method called Freeform Fabrication (FFF), although in a more condensed fashion. All subsequent incarnations of the RepRap platform, including open source and commercial models, utilize extrusion technology.

It is uncertain how the entry-level section of the market will change moving ahead, though, as all of the machines might be at risk for patent infringements after Stratasys launched a lawsuit against Afinia.

A heated extruder is used in the method to melt plastic filament applied to a build platform one layer at a time in accordance with 3D data sent to the printer. When more layers are added, they get tougher and link to the ones that came before them.

Stratasys has produced a number of distinctive artificial- grade accoutrements using their FDM system that are suitable for a range of product requirements. At the morning of the request, accoutrements are more limited, albeit the range is growing. ABS and PLA are the most frequent corridor used in entry- position FFF printers.

Support structures are necessary for the FDM/FFF operations in any applications with overhanging geometry. This necessitates the use of a second, water-soluble material in FDM, which, after the print is complete, permits support structures to be rather easily removed. It is also possible to employ breakaway support materials, which may be removed from the component by physically snapping them off. The support structures, or lack thereof, of the entry-level FFF 3D printers has traditionally been a limitation. Nonetheless, it has become less of an issue as the systems have grown and changed to accommodate double extrusion heads.

Although the FDM method from Stratasys normally works well in offices and studios and generates models with precision and reliability, significant post-processing may be required. As

predicted, the FFF approach initially produces models that are substantially less accurate, but things are constantly improving.

Layer-to-layer adhesion may be difficult for particular component shapes, slowing down the process and producing components that are not waterproof. Again, acetone post-processing can solve these issues.

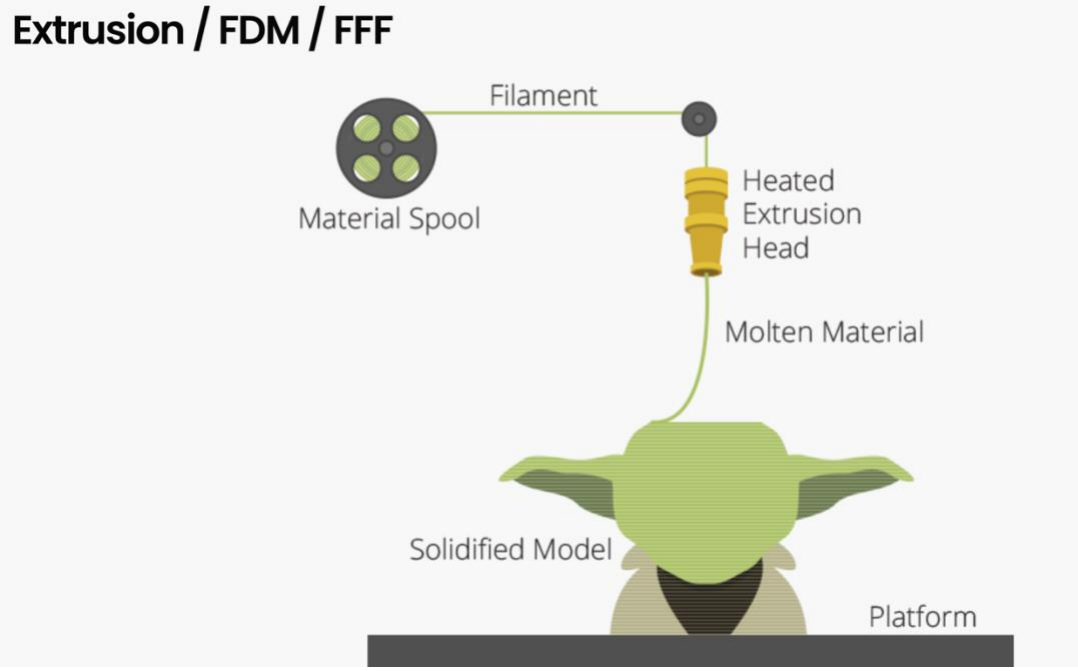

Figure 2 Extrusion

SDL

Mcor Technologies evolved and manufactures SDL, a special 3D printing fashion. It's tempting to compare this process to Helisys' Laminated Object Manufacturing(LOM) technology from the 1990s because both bear mounding and putrefying paper to produce the finished product. nonetheless, there's no more similarity. The SDL 3D printing process generates factors subcaste by subcaste using ordinary dupe paper. Each posterior subcaste is attached to the one before it using an glue that's applied widely in agreement with the 3D data given to the machine. As the region that will come the element is placed with a significantly advanced viscosity of tenacious than the girding area, which will serve as the support, this enables fairly easy" weeding" or support

junking. Once a new distance of paper is put into the 3D printer via the paper feed medium and placed on top of the preliminarily applied cement that was applied just to certain places of the previous subcaste, pressure is given to the figure plate, which is pushed up to a heat plate. This pressure causes the two wastes of paper to appreciatively bind. The figure plate slides back to the figure height as the edges of the item are constructed using a Tungsten carbide blade that's customizable. After this slice cycle, the 3D printer will apply the coming subcaste of cement, and so on until the part is complete.

Selective Deposition Lamination is one of the few 3D printing processes that can manufacture components using a CYMK color scheme in full color. The pieces don't require any further processing because they are made of normal paper and are fully safe and ecologically friendly. The method falls short of other 3D printing technologies in two aspects, namely the manufacturing of complex geometries and the construction size being limited by the amount of material.

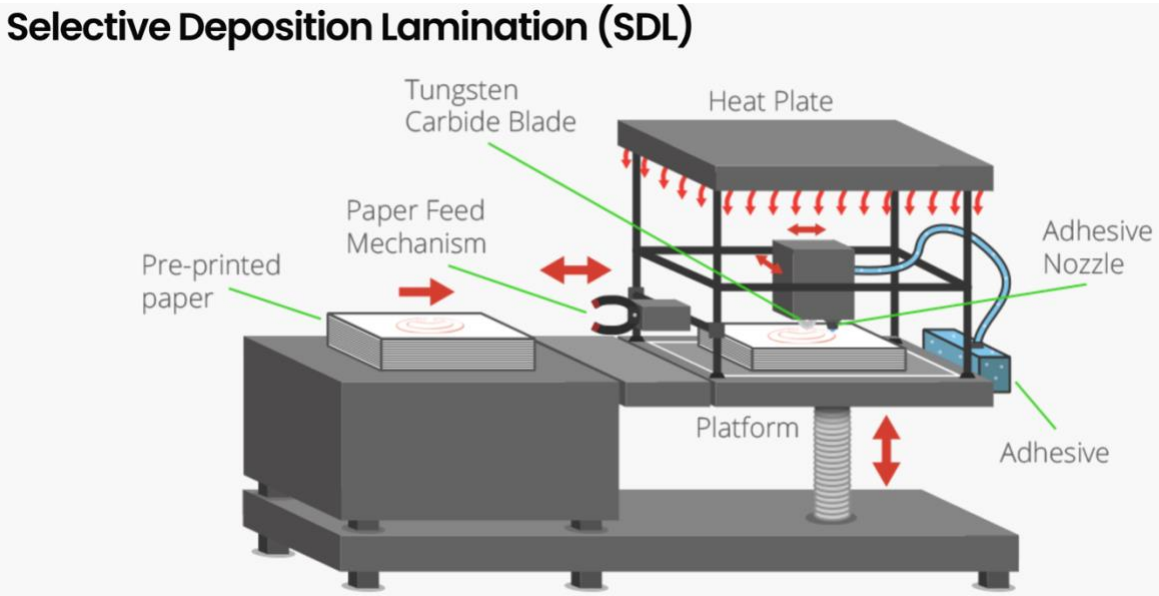

Figure 3. Selective Deposition Lamination

EBM

The personalized process for 3D printing with electron ray melting was developed by the Swedish company Arcam. This system of essence printing is veritably analogous to the Direct Metal Laser Sintering(DMLS) process for producing effects from essence greasepaint. The crucial difference

is that the process requires a vacuum since it uses an electron ray as its heat source rather than a ray, as the name indicates. EBM's capability to make completely- thick factors in a variety of essence blends, indeed to medical grade, has proven particularly useful for a range of manufacturing operations in the medical assiduity, especially for implants. In malignancy of this, other high- tech sectors including aerospace and automotive have also sought to EBM technology for product fulfillment.

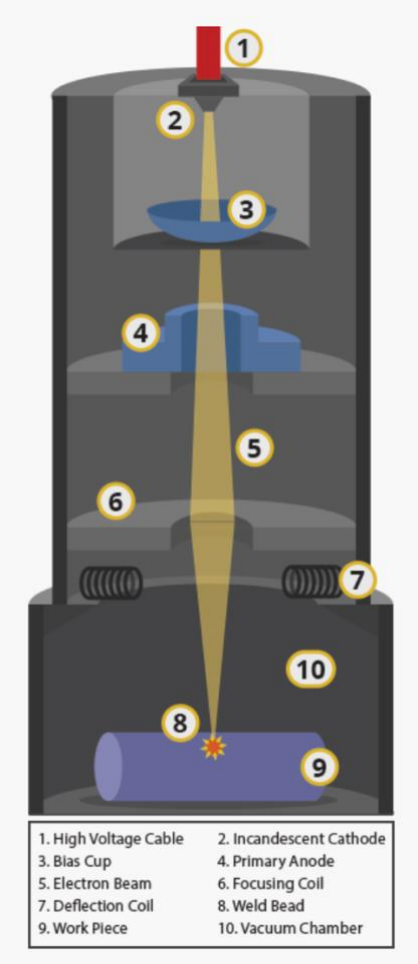

Figure 4. Electronic Beam Melting

Materials

Plastics

Nylon, or polyamide, is widely used as filament in the FDM process and as powder in the sintering process. Due to its durability, malleability, and strength, it is a reliable plastic for 3D printing. While it is white by default, coloring is an option both before and after printing. Alumide, a well-

liked 3D printing material for sintering, may be made by combining this chemical (in powder form) with aluminum powder. ABS is another well-liked substance for 3D printing, and entry-level FDM printers typically utilize it as filament. It is a material that is quite resilient and is offered in a variety of hues. The accessibility of ABS in filament form from a range of non-proprietary sources is another factor in its appeal. The biodegradable plastic material PLA has grown in fashionability with 3D printers just for this reason. It may be employed in resin format for the DLP/ SL processes as well as hair format for the FDM process. It comes in a variety of colors, including transparent, which has shown out to be a useful option for several 3D printing operations. It isn't, still, as robust or flexible as ABS.

LayWood is a material that was developed particularly for 3D printing and is suitable for entry-position extrusion printers. It's a compound material that comes in hair form and is constructed of wood and polymer(also appertained to as WPC).

Metals

Essence and essence mixes are decreasingly used in artificial- grade 3D printing. The two most common bones are cobalt and aluminum derivations. One of the strongest and most frequently used essence for 3D printing is pristine sword in greasepaint form for the sintering, melting, and EBM processes. Although being naturally tableware, it may be carpeted with different accoutrements to give it a gold or citation appearance.

Recently, the list of metals that may be 3D printed has expanded to include gold and silver, both of which have obvious applications in the jewelry business. Both of these minerals are strong and may be processed into powder. Titanium, one of the toughest metals, has long been used in commercial 3D printing applications. It is offered in powder form and is suitable for sintering, melting, and EBM operations.

Ceramics

Pottery are a fairly new class of accoutrements that are used in 3D printing with variable degrees of effectiveness. The unique aspect of these accoutrements is that the ceramic pieces need to go

through the same processes as any ceramic element produced using conventional manufacturing ways, most specially fire and glazing, after printing.

1.2 Melt Extrusion

During the nonstop high volume product process known as plastic extrusion, also known as plasticating extrusion, a thermoplastic material, whether it be in the form of greasepaint, bullets, or granulates, is homogeneously melted. The material is also forced under pressure out of the shaping bones. As a screw is extruded, pressure is produced when the screw rotates against the barrel wall. When the plastic melt has gone through the bones and assumed the shape of the bones hole, it comes out of the extruder. The extruded product is appertained to as an extrudate.

There are typically four zones on an extruder:

Feed Area

This region has a constant flying depth. The flight depth is the distance between the screw's main diameter at its top and its minor diameter at its lowest.

Compression zone or transition zone

At this point, the flight depth begins to decrease. In a sense, the thermoplastic material gets compressed and begins to plasticize.

Mixing Area

Once more, the flight depth remains constant in this region. To ensure that the material is completely melted and combined, a specialized mixing component may be utilized.

Metered Area

While it is constant, the flight depth in this zone is lower than it is in the mixing zone. Moreover, the pressure in this region pushes the melt through the shaping die.

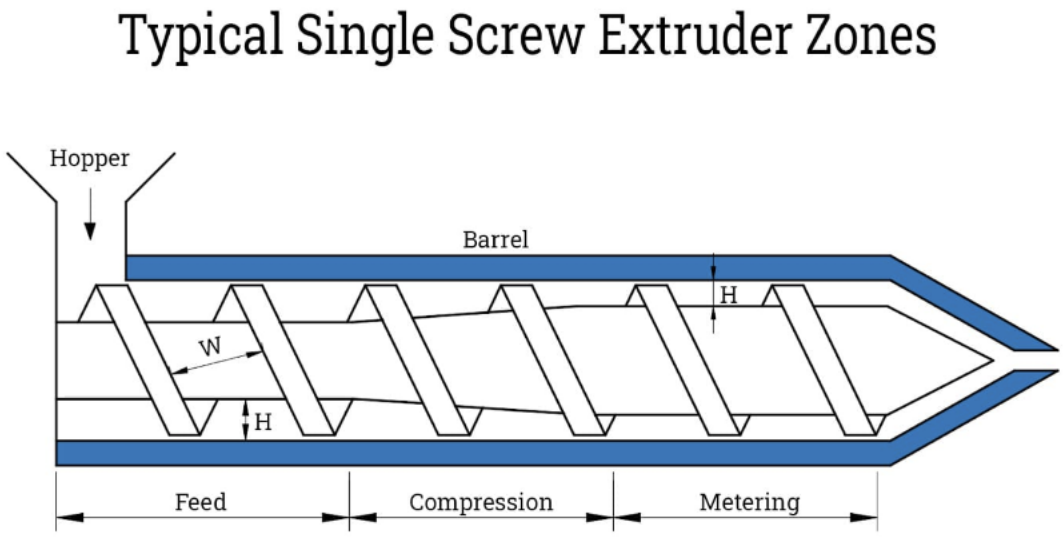

Figure 5. Single Screw Extrusion

In addition, there are three main reasons why the polymer mixture melts:

Heat Exchange

Heat transfer is the process by which energy is transferred from the extruder motor to the extruder shaft. Moreover, the screw profile and dwell time affect polymer melting.

Friction

The screw profile, screw speed, and feed rate, together with the internal friction of the powder, all contribute to this.

Barrel of extruder

The barrels' temperature is maintained using three or more separate temperature controls.

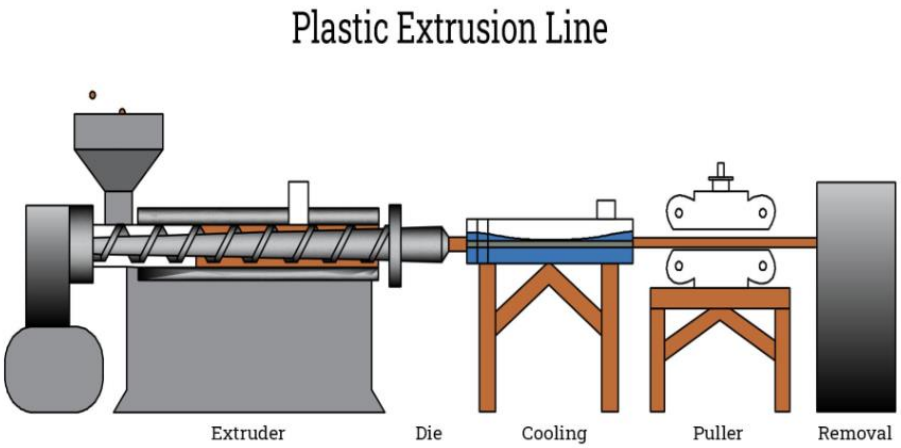

Figure 6. Extrusion of Plastic

1.4.1 Basic Processes

Prior to the main extrusion process, the stored polymeric feed is mixed with a number of complements to ameliorate the product quality and processability. These complements include stabilizers(for heat, oxidative stability, UV stability, etc.), color colors, honey retardants, paddings, lubricants, mounts, etc. To get the applicable property profile characteristics, a polymer can be given complements.

For some resin systems, a fresh drying process is generally employed to help the polymer from demeaning due to humidity. Even if a material often doesn't need to be dried before use, it could still. This is especially true if the item was recently relocated from a cold location to a warmer one, which caused moisture to condense on the material's surface. Once the polymer and additives have been mixed, dried, and fed, the mixture is gravity fed down the extruder throat and into the feed hopper.

Solid materials' flowability, such the flowability of polymer powder, is a common problem. Several situations might lead to material bridging inside the hopper. Hence, further efforts can be taken to prevent any polymer accumulation on the feed hopper's surface and guarantee appropriate material flow, such as the sporadic injection of nitrogen or another inert gas.

By flowing upwardly, the material enters the annular space between the screw and the barrel. The substance is also contained by the screw channel. When the screw rotates, the polymer is propelled forward and is subordinated to frictional forces. Generally, the temperature profile used to toast the barrels grows gradationally. The material is plasticized, fully mixed, and sculptured together as it passes from the feed zone up to the metering zone due to frictional forces and barrel heating. As the melt approaches the extruder's terminal, it first passes through a screen pack. With the screen pack, the thermoplastic melt is fully filtered of any extraneous factors. also, it avoids the bones plate hole from being congested. The melt is also forced out of the bones to induce the bones shape. It's fleetly cooled and pulled out from the extruder at a harmonious speed. farther processes, similar as honey treatment, printing, cutting, annealing, deodorization, etc., can be done aftercooling. However, the extrudate will next suffer examination before being packaged and dispatched, If every criterion for the product is met.

1.4.2. Types of extruders

Today's market offers extruders in a variety of designs. Depending on the way of operation, they can be split into two categories:

1. continuous extruders
2. inconsistent extruders

The component that transports the material often distinguishes the two. Discontinuous extruders have components that reciprocate, whereas continuous extruders have rotating parts.

You may further classify continuous extruders into two categories:

1. extruders for screws
2. extruders with disks or drums

Single Screw extruder

Because of its multitudinous advantages, similar as their low cost, straightforward design, durability, responsibility, and outstanding performance/ cost rate, single screw extruders are the most extensively used nonstop extruders in the polymer extrusion assiduity.

There are three zones in a typical single screw extruder that differ geometrically ; Feed Zone Transition, Metering Zone, or Compression Zone The three zones are caused by the screw's channel depth, which changes but has a constant pitch.

From the feed zone to the metering zone, the screw channel depth linearly decreases, which results in the contraction marvels. When pertaining to screw designs with only one contraction section, it's constantly called a single stage. Zone length and outside and minimal channel depths may vary with the same screw length and periphery.

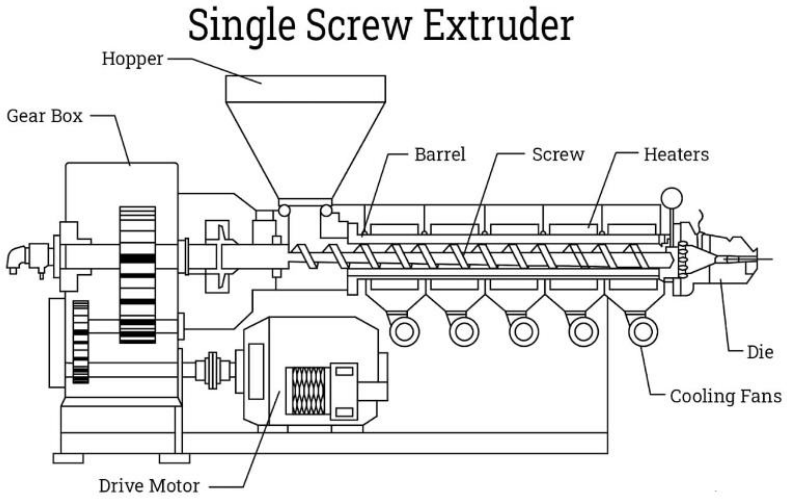

Figure 7. Single Screw Extruder

The following elements may also affect the thermochemical conditions inside the extruder:

1. temperature screw profile
2. screw rate
3. local heat conduction, heat dissipation, velocity profile, and residence duration inside the extruder are all impacted by these variables

The typical configuration of single screw extruders includes:

1. heating elements—used to control the barrel's axial temperature profile
2. upstream of the extruder is the feed hopper and entrance
3. die is situated at the extruder's opposite end

Twin Screw extruder

Continuous multiple screw extruders are a common classification for twin screw extruders. Since they are constructed with two Archimedean screws, these extruders get their name. As various design elements, such as rotational direction and degree of intermeshing, may be changed in twin screw extrusion, there are several distinct varieties of twin screw extruders.

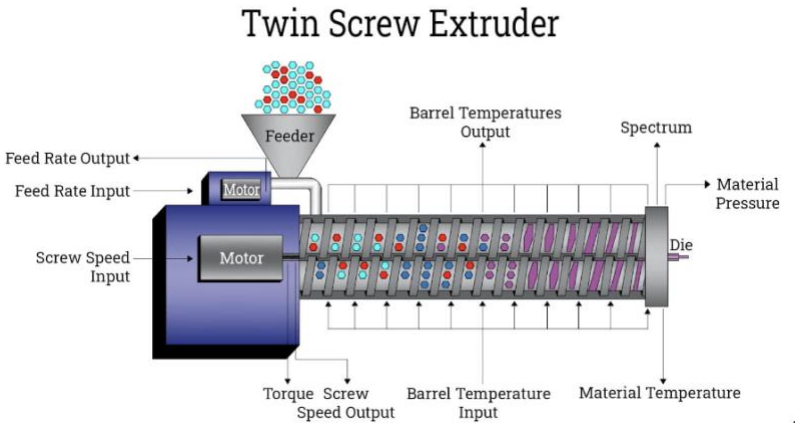

Figure 8. Twin Screw Extruder

They could be further classified into:

Intermeshing extruders

   a. co-rotating extruders
   b. counter-rotating extruders
2. non-intermeshing extruders
   a. counter-rotating extruders
   b. co-rotating extruders
3. co-axial extruders

Multi-Screw extruder

An extruder with further than two screws is generally shown by the planetary comber extruder. This extruder has a single screw extruder- suchlike characteristics, especially in the feed area. But, the mixing step is where the difference is first made. In the planetary comber part, there are six or further unevenly spaced planetary screws girding the main screw, also known as the sun screw. The barrel, the planetary screws, and the sun screw interact. This section of the barrel has spiral grooves erected into it to accommodate the spiral breakouts of the planetary screws. The feed part and the planetary comber section are generally connected via a flange- type connection.

Planetary roller extruders can actively combine materials because of the rolling motion created by the planetary screws, sun screw, and barrel. The advantage of this extruder is that it can handle heat-sensitive materials with minimum deterioration.

Planetary roller extruders are frequently used to extrude PVC that is stiff or plasticized. It may also be included into conventional extruders to improve their mixing capacities.

Disk Extruder

Despite the fact that they do not use screws to move the material, disk extruders are classified as continuous extruders. They use disks or drums as an alternative to speed up the extrusion process. In some cases, the term "screwless extruders" is also used to describe disk extruders. Most disk extruders function by transferring drag in a viscous medium.

Stepped Disk Extruders

Stepped Fragment extruders, also known as slider pad extruders, place a flat fragment conterminous to a stepped fragment. Pressure is generated at the gap size change when one of the disks is rotated with a melt in the axial gap.

Stepped fragment extruders can be used in a nonstop process if the stepping fragment contains erected- in exit channels. One of this extruder's biggest downsides is its maintainability. The intricate layout of the inflow channels makes drawing delicate.

Drum Extruder

The barrel extruder works to banish material using a rotating barrel and barrel. The polymeric material is pumped into the annular space between the barrel and the barrel. The material is moved around the barrel's circumference as the barrel rotates. Just previous to a full gyration, there's a wiper bar that removes melt from the barrel and directs the inflow to the exit and also to the extruder bones.

Diskpack Extruder

When it comes to executing basic polymer processing tasks, diskpack extruders are just as efficient as traditional equipment. Drum and single screw extruders both have features in common with it. Diskpack extruders are single screw extruders with very deep flights and no helix angle.

The material is pushed into the space between two thin disks on the rotating shaft. A channel block closes the space between the disks before one complete rotation. The disks and the melt move together. This channel, analogous to the wiper bar in barrel extruders, directs the inflow to the affair channel.

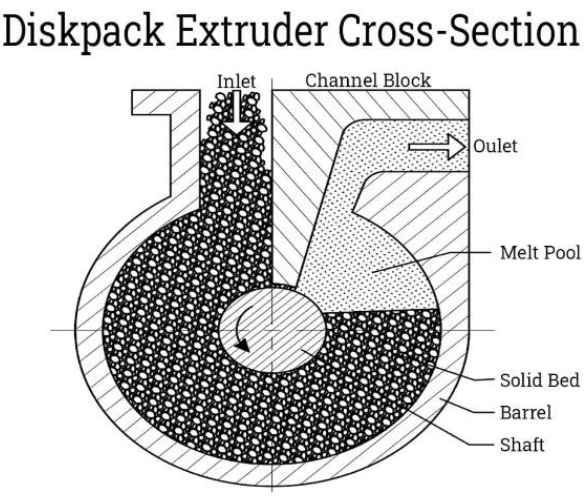

Figure 9. Diskpack Extruder

Elastic Melt Extruder

In discrepancy to traditional fragment extruders, which calculate largely on thick drag transport, elastic melt extruders use the elastic parcels of polymer melt to move the material and give the needed bones head pressure. When the material is sheared between stationary and rotating plates, an uneven distribution of normal stresses will show in the melt.

These pressures give a centripetal pumping stir that propels the nonstop extrusion of material via a central opening. Normal stress extruders are another term for elastic melt extruders because of this procedure.

1.3 Additives

Cellulose Nano-fibers

The most advanced biomass material in the world is made of cellulose nanofiber, which is made from wood-derived fiber (pulp) that has been defibrillated to a nano level of several hundredths of a micron and smaller. Because it is created from plant fibers, the material has less impact on the environment during both production and disposal. Its outstanding features include its low weight, an elastic modulus equivalent to high-strength aramid fiber, thermal expansion comparable to glass, and strong barrier capabilities for gases such as oxygen.

Characteristics

Cellulose nanofiber is regarded as a possible material for use in a number of industries, such as filter material, high gas barrier packaging material, electrical devices, foods, medicines, cosmetics, and health care. This is as a result of its distinctive form and physical attributes.

Businesses have been successful in commercializing incredibly effective antibacterial and deodorant sheets using the CNF with TEMPO catalytic oxidation technique. Nippon Paper Crecia Co., Ltd., a Group company (President: Yasunori Nanri), launched the "Hada Care Acty" line of adult diapers as the first product made from useful CNF Sheets. Also available from Crecia is the "Poise" series, a mild incontinence pad made from the same CNF sheets.

Some of CNF's characteristics are as follows:

1. light and powerful
2. very fine fibers (fiber width: about 3 nm)
3. substantial specific surface
4. little thermal expansion.
5. strong gas barrier capabilities
6. demonstrates typical viscosity in water
7. biomass that is favorable to the environment

Problem Statement and Motivation

The primary idea behind this thesis is to create composite filament for FDM printing employing nano additions to achieve improved mechanical properties. PLA was selected as the host substrate polymer because it is often used in 3D printers and is simple to replace with different polymers. The host polymer substance was picked out to include CNF as an addition. Producing conductive filament for FDM printing is made possible by the unique properties of CNF, which increase the mechanical strength of the host polymer. This filament may be used to print products with better mechanical properties across a range of industries, including the automotive, aerospace, and bio-medical sectors. (Figure 9)

Figure 10. Melt Extruded Filament

1.4 Overview

Nanocomposite filaments were produced in this thesis via melt extrusion. As discussed in chapter 1, melt extrusion was used to make PLA composites so that filament could be made from them. Chapter 2 reviews a number of nanocomposites along with their improved properties and manufacturing processes. The precise manufacturing procedure for the PLA nanocomposite is covered in Chapter 3. SEM, Raman, FTIR, and material characterization techniques were used to assess the mechanical properties of the generated filaments. The aforementioned information was utilized to examine how CNF distributed in the polymer matrix. The features of the produced filament samples are compared in chapter 4 to those of commercially available filaments and filaments currently under development in research institutions. The conclusion of the thesis is provided by Chapter 5.

2. LITERATURE REVIEW

The nature of cellulose and its common forms, notably cellulose nanofibrils (CNF) and cellulose nanocrystals, are examined in this chapter (CNC). In order to provide the reader with a context for comparison and a comprehensive understanding of current technology, bacterial cellulose (BC) is briefly mentioned.

2.1 Cellulose

Cellulose, the most prevalent biopolymer in the world, is present in plants, algae, fungus, minerals, and mammals [25]. The middle layer of the secondary wall, one of the layered extracytoplasmic structures present in plant cells, helps to preserve the stiffness and structure of the cell [26]. The layer of lignocellulosic fibers in Figure 10 is made up of cellulose microfibrils that are encased in a polysaccharide and glycoprotein matrix, as well as lignin and pectin [26]. Inorganic salts and waxes are among the non-structural elements found in the compact fiber. The cleanest source is cotton fibers, which have a crystallinity of about 70% and a cellulose content of 95–97%. According [27]and[28], lignin and other polysaccharides known as hemicelluloses make up a significant portion of the stems of birch and pine trees, which comprise about 40% cellulose.

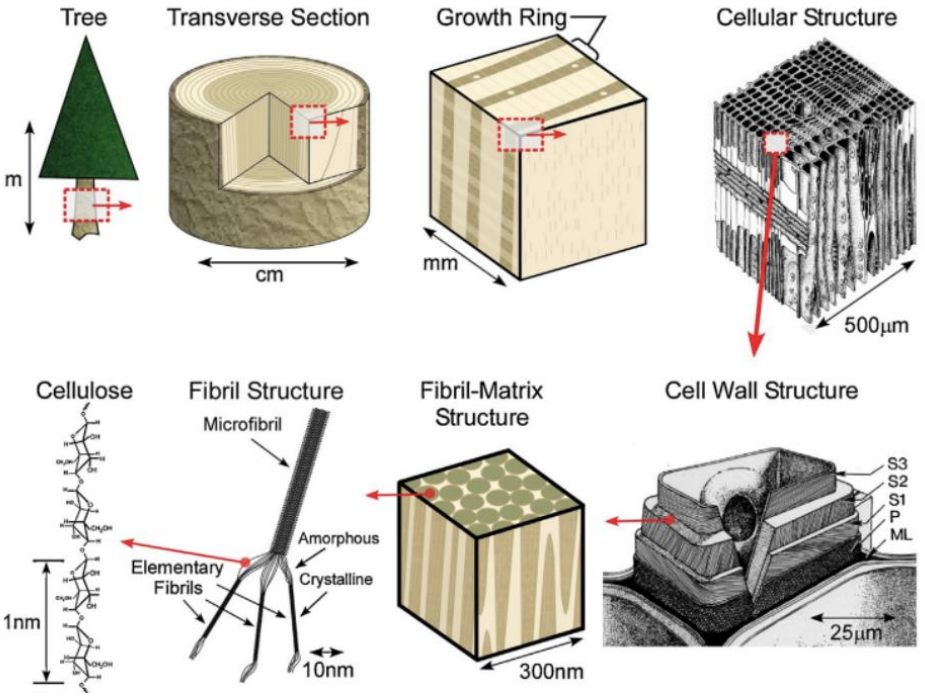

Figure 11. Cellulose

The molecular structure of cellulose is independent of the source, however the chain length varies depending on the source and other elements like age, soil type, growing conditions, and botanical origin alter the chemical makeup of the raw fibers. The primary fibrils of cellulose are formed by the natural biosynthesis of between 30 and 100 molecules joined together [26]. It has been suggested that the first biopolymers to develop on earth were carbohydrates [29]. Prior to the discovery that the molecular arrangement had little to do with water, all substances having the general formula C_xH_2O were first believed to be "hydrated carbon" [29]. Polysaccharides' components, structure, and bond type all affect how they behave.

For instance, combining the two sugars fructose and glucose results in sucrose, a kind of table sugar. Via condensation processes, wherein one monomer loses a hydrogen atom and the other monomer loses a hydroxyl group, disaccharides are created in the cell. Covalent glycosidic linkages that arise in two instances—alpha and beta—then join them together. Among their many uses, sugars are crucial for the storage of energy in cells [29].

Whereas structural polysaccharides naturally develop extended forms with steric limitations on the rotation of monomers, storage polysaccharides frequently form helical shapes. French chemist "Anselme Payen" first identified the chemical makeup of cellulose in 1838, estimating that it is composed of 44–45% carbon, 6–6.5% hydrogen, and 0.6–0.7% oxygen, giving it the formula $C_6H_{10}O_6$ [30].

Haworth made the initial suggestion for the macromolecular chain structure in the late 1920s, and Staudinger later confirmed it. The D-glucopyranose units are made up of six-membered rings connected by β-1,4-glycosidic bonds that have five carbons and one oxygen atom in the lowest energy state, or $^4C_1$-chair configuration [31]. An anhydroglucose unit is a ring with three reactive hydroxyl groups at positions C_6, C_2, and C_3 (AGU). As seen in Figure 11, bonding forces every other ring to spin 180 degrees along the chain axis to create a linear syndiotactic homopolymer. Strong hydrogen bonds cause high crystallinity, little solubility, and significant hydroxyl group reactivity.

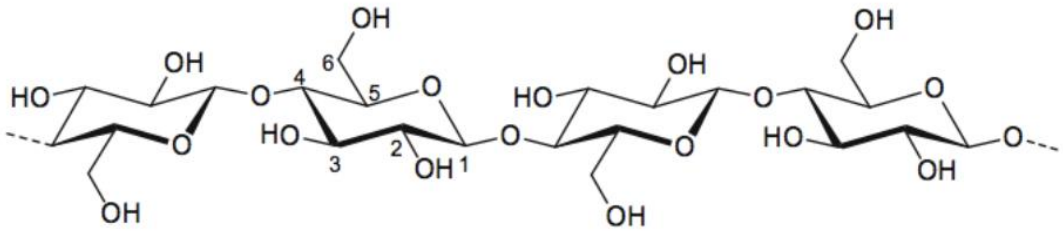

Figure 12. Structure of Cellulose

There are four different types of cellulose that have been linked, with crystalline native cellulose, or cellulose I, being the most current and set up in lignocellulosic shops[28, 29]. The fibril structure of the cellulose macromolecules can be separated between areas of so- called unformed sections with low crystallinity and high order crystalline regions because the macromolecules aren't dispersed slightly throughout [28].

2.1.1 Nano-cellulose

In accordance with a standard established by the European Commission [32] in October 2011, materials are categorized as nanomaterials if 50% or more of the particles have at least one exterior dimension less than 100nm [32]. Since the manufacture began in the late 1970s, the definition of nanocelluloses has been diverse, although standards have subsequently been suggested and some acronyms have become more common [31]. According to its dimensions and production methods, nanocellulose from vegetal sources can be classed. Figure 3 illustrates some of the existing acronyms and names for this material [33]. In this paper, cellulose nanocrystals and nanofibrils are abbreviated CNC and CNF, respectively.

Table 1. Common Abbreviations

Processes	Abbreviations	Synonyms
Mechanic	**CNF**, MFC, NFC	**Cellulose nanofibrils**, nanofibrillated cellulose, cellulose microfibers, fibrillated cellulose.
Chemical	**CNC**, CNW, NCC	**Cellulose nanocrystals**, whiskers, crystal of cellulose, crystalline nanocellulose.

2.1.2 Cellulose nanofibers (CNF)

Softwood pulp's enhanced viscosity after numerous passes via a homogenizer was found in 1983. [34]. Depending on separation techniques, processing intensity, and source, CNFs—which are typically separated using top-down approaches without any enzymatic or chemical treatments—have significant width and length differences in their properties. Because of this, characterization is challenging [31]. The bundles of constituent fibrils that make up the CNFs generally have widths of 20 to 50 nm and lengths of 500 to 2000 nm [35]. They have a specific surface area of 100-200 $m^2 g^{-1}$ and a crystallinity of 60 to 70%. [31].

Comparing CNF to CNC and bacterial cellulose (BC), it has the advantage of being more readily generated in commercial numbers and being suitable for a larger range of uses [36]. Due to its qualities, CNF can be utilized as a reinforcement in composite materials, paper and board, rheology modifier in products like cosmetics, a food additive, or to increase barrier properties in packaging [31]. Since CNF can self-assemble to produce thick films with strong barrier qualities, fully green packaging materials are a viable use for it [37].

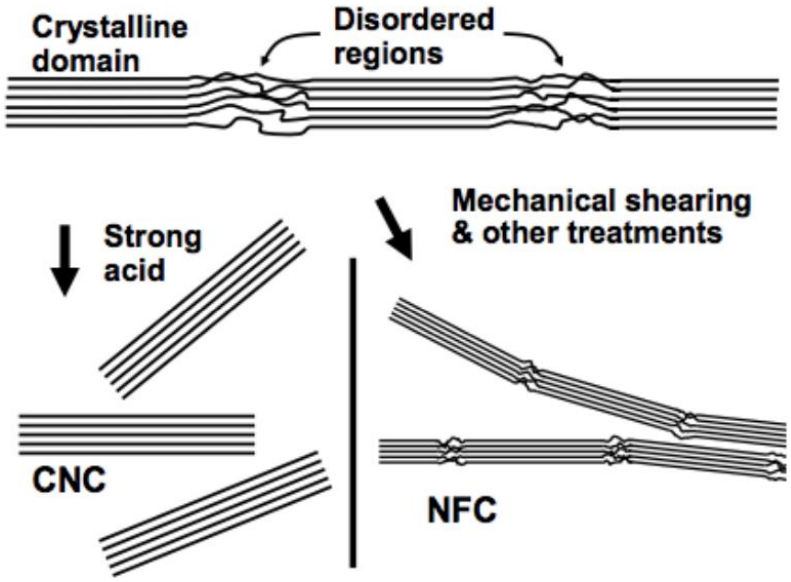

Figure 13. CNC and CNF

Cellulose Nano Crystals (CNC)

It took the introduction of acid hydrolysis for crystalline areas to be separated from fibers [28] Strong acids are used in selective degradation to eliminate the amorphous portions while keeping the highly organized sections untouched. Typically, 25 to 75% of biomass-derived cellulose is crystalline, and isolated CNCs have crystallinities that are less than 80%. [34]. If these extremely crystalline areas were transferred to a composite, it would provide enormous load-bearing mechanical qualities that reach the theoretical modulus of a perfect crystal (138–150 GPa) [26]. The surface area of the suggested CNCs is 150–250 m^2 g^{-1} [35].

[28] asserts that the majority of researchers share a misunderstanding regarding the type and proportion of crystalline and amorphous areas in cellulose nanofibrils. This group contends that

the amorphous components might be viewed as flaws in the crystallites because of their vastly dissimilar characteristics and prevalence of the unordered areas.

Amorphous areas in ramie fibers that only cover four to five AGU (1.5% of the total mass), according to [28], are too tiny to be compared to bulky amorphous regions in artificial semi-crystalline polymers.

2.1.3 Bacteria Nanocellulose (BC)

Bacteria that produce chemically pure cellulose are used in a bottom-up nanocellulose production technique, and it is this purity that sets BC apart from plant cellulose. Only the Acetobacter species has been seen to generate sufficient amounts of cellulose for commercial use. The fermentation of sugars and plants produces this amazing non-photosynthetic organism, which can turn ethanol into acetic acid and carbohydrates into cellulose [29]. The production of cellulose is thought to provide defense against outside dangers and function as a flotation mechanism to ensure the availability of oxygen, which is essential for the organism. Additional hypothetical uses include UV light protection and moisture absorption. The most researched species of Acetobacter, Acetobacter xylinum, which obtains sugars, is also known as Gluconacetobacter. It is available for purchase from international collections of microbes [29].

Table 2. Products of Cellulose

Genus	Cellulose structure
Acetobacter	Extracellular pellicle composed of ribbons
Achromobacter	Fibrils
Aerobacter	Fibrils
Agrobacterium	Short fibrils
Alcaligenes	Fibrils
Pseudomonas	No distinct fibrils
Rhibozium	Short fibrils
Sarcina	Amorphous cellulose
Zoogloea	Not well defined

2.2 Manufacturing of CNF

The raw material that will be utilized determines where the production process will begin. In order to skip the task of eliminating undesired non-cellulosic contaminants, bleached pulps are frequently used [29]. Raw fibers must undergo a source-dependent chemical treatment if that is the starting material chosen. The raw biomass is pulverized in a general method outlined by [29] to improve surface area and enhance accessibility, and waxes are periodically removed using a soxhlet equipment with a solvent combination. Water-soluble polysaccharides are eliminated after the wax removal process using an alkali treatment using 2% NaOH solution at 80 °C.

Following washing and removing the byproducts, sodium chlorite (NaClO2) is used to bleach the remaining polysaccharides, such as lignin, proteins, and polyphenols. This process should produce a material that only has the cellular structure [29].

2.2.1 Treatments using enzymes and chemicals

Before attempting to physically isolate the constituent fibers, nature-inspired enzymatic and chemical pretreatments can be utilized to lower the bonding energy [38]. In the majority of chemically assisted methods, anionically charged functional groups are introduced to facilitate the fibrillation of wood, cotton, bacterial, and tunicate celluloses by creating repulsion between the water and fibrils. The term "tempo-mediated oxidation" (TEMPO), which stands for the utilization of 2,2,6,6-tetramethylpiperidine-1-oxyl radicals, refers to a successful therapy. This procedure selectively converts C_6 primary hydroxyls to carboxylate groups to separate elementary nanofibrils from native wood fibers while altering the surface chemistry [39]. The Ames test, which determines mutagenic activity, yields largely negative results for these commercially available nitroxyl radicals.

This is important because it may be used safely to make a range of consumer particulars. In nature, cellulose is efficiently broken down by enzymes, and filaments with well- saved molecular weight and length have been produced by controlled decomposition at incredibly low enzyme attention

[38]. Acid hydrolysis treatments drastically dock filaments by dissolving unformed regions, and inordinate hydrolysis results in short, low- molecular- weight CNCs[40].

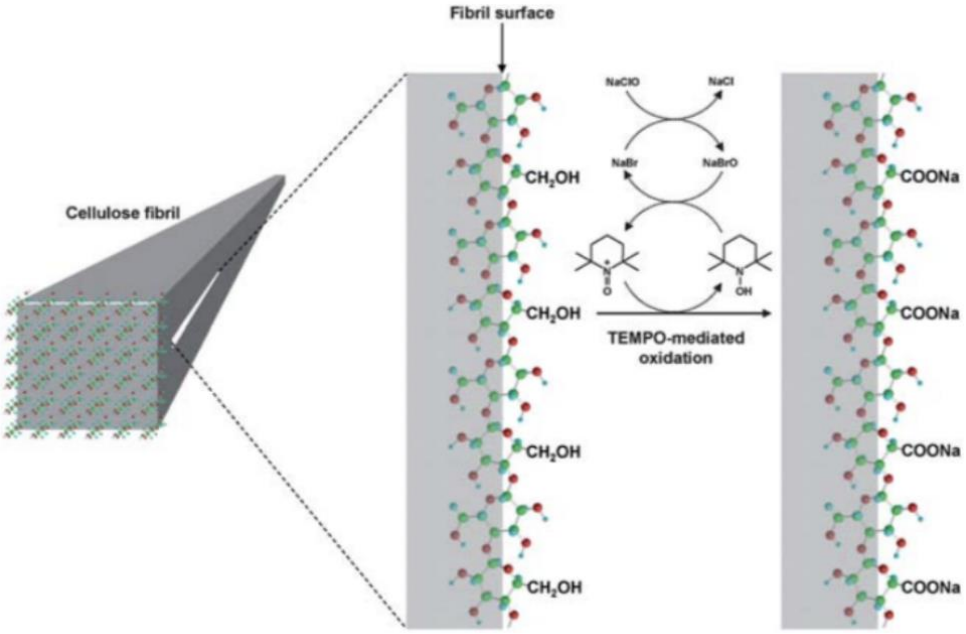

Figure 14. Process of Oxidation [39]

2.2.2 Mechanical Treatment

To produce CNF, top-down techniques delaminate cellulose microfibers [41]. The physically intensive mechanical processes use strong shear pressures to separate the microfibrils into the substructures seen in Figure 10 by rupturing intermolecular hydrogen bonds [29]. It is difficult to isolate elementary fibrils, and it is impossible to do so without suffering significant mass losses [39]. Treatment may fail to entirely dissolve the fibers, harm the structure, or diminish crystallinity [40]. Top-down separated cellulose has a degree of polymerization (DP) between 800 and 3000. [31].

Homogenization, grinding, or micro fluidization are the three methods that mechanical fibrillation is most frequently carried out by, but it can also be carried out solely by chemical treatment, high intensity ultra sonification processes, or chemical/enzymatic treatments followed by mechanical

fibrillation [41,42]. Compared to pure mechanical therapies, chemically aided mechanical fibrillation uses a lot less energy [31]. By driving an aqueous solution through a slit while applying pressure differentials, cavitations, and shockwaves to the cellulose fibers, traditional high-pressure homogenization techniques created in the 1980s function [31,35]. Static pressure decreases while velocity and dynamic pressure rise as the suspension is driven through the slit.

Gas bubbles occur as a result of this decrease below the water's vapor phase, and when they reach normal air pressure, they burst. The pressure ranges from 50 to 2000 MPa, while the gap width is based on viscosity and ranges from 5 to 20 μm. [35] Several runs through the homogenizer are necessary for the suspension to attain an appropriate fibrillation, which also raises the energy consumption [40]. The rather sophisticated gear can lead to blockage, which would be detrimental to the process's already high energy and time costs [31]. According to [35], high processing intensity degrades the crystalline structure.

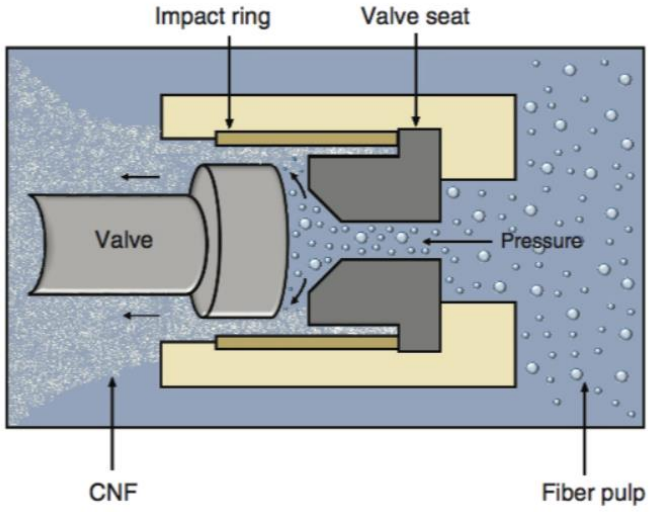

Figure 15. Process of homogenizing pulp to minimize size

When the suspension is injected into a small channel with abrupt twists (typically z-shaped), microfluidizers work at a constant shear rate, degrading the fibers as they hit the channel walls (Figure 14). The machine's construction enables the suspension to be circulated to enhance effectiveness [35]. In contrast to the traditional homogenization method, this is more effective and

needs less cycles (5–20 cycles), and the lack of moving components also reduces the likelihood of clogging. [31] makes these arguments.

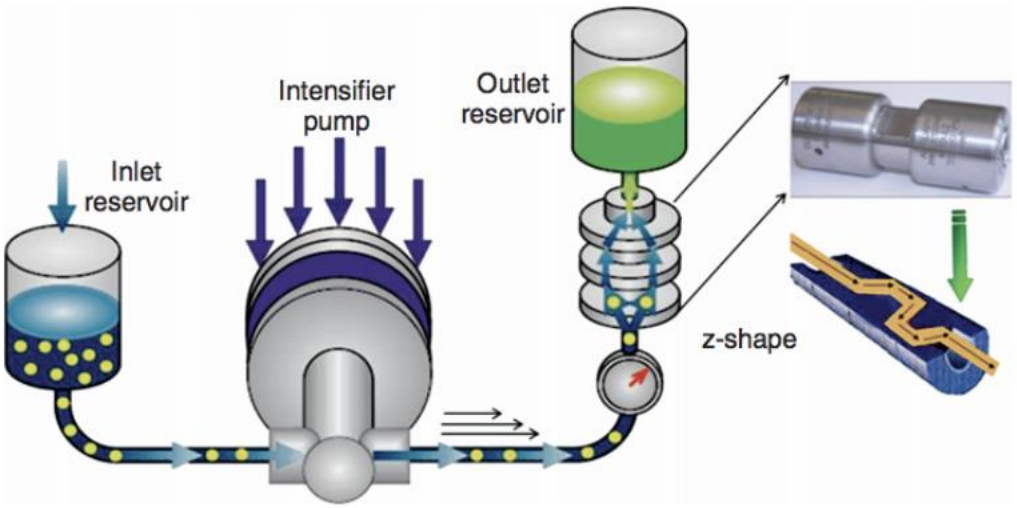

Figure 16. Microfluidizer [38]

The grindstones in Figure 16 are used by grinders to mechanically fibrillate cellulose [38]. The resultant particle size depends on the movable distance between the stones, which is adjustable, and rotates at a speed of around 1500 rpm relative to the other two grindstones [35]. The requirement to repeat the operation several times makes it challenging to monitor pulp consistency due to water evaporation brought on by friction.

Figure 17. High intensity grinder

2.2.3 Methods for Drying

The majority of CNF composites must be prepared without liquids, which presents a challenge because the bulk of cellulose processing is done in aqueous solutions [33]. Evaporation and lyophilization are two frequently used drying techniques. [33] split the evaporation process into the following three steps: a phase of steady evaporation followed by a decrease in drying rate. The second stage occurs when the suspension's vapor content begins to dissipate and the fibers' movement becomes constrained. When the distance between particles is minimized and submolecular interactions take place, the process is complete. Reactive hydroxyl groups cause intermolecular hydrogen bonds to form, which are both irreversible and somewhat reversible, when the particles are brought together. The history of this procedure, known as hornification, in the paper and pulping business is extensive [43].

These fiber clusters are challenging to separate, and after drying, the solution loses its original inflated form. Lyophilization, commonly known as freeze-drying, is the second and simplest method of eliminating water without compromising the structure and volume of the object [33].

This method removes the water by first freezing the aqueous solution and then turning it into water vapor at pressures below the water's triple point and temperatures between -20 °C and -50 °C.

2.3 Modification of CNF

In many instances, the cellulose's hydrophilic properties brought on by the hydroxyl groups are troublesome. Many benefits of surface changes include drying without aggregation and increased compatibility with a larger range of matrix materials. It is still common practice to chemically modify the hydrophilic hydroxyl groups in order to reduce surface polarity and enable uniform dispersion in nonpolar fluids [44]. The anticipated percolation effects "insulating" the components from one another might be defeated by an excessive degree of substitution, though [45]. This section discusses a few popular methods for modifying cellulose to make it more hydrophobic.

2.3.1 Chemical Grafting

The hydrophobicity of cellulose is increased during esterification processes using acid anhydrides, carboxylic acid, or acid chlorides as reacting agents. This has been shown to be successful in enhancing the dispersion of CNF and CNC in nonpolar mediums and significantly reducing the amount of aggregates [46,38]. Mechanical fibril isolation may be done either before or after acetylation, and pre-isolation therapy has no discernible deleterious effects on the degree of substitution (DS) [47]. Understanding this, it is more effective from a production standpoint to modify the wood pulp before fibrillation [48].

The main hydroxyl groups are esterified during the acetylation step using acetic anhydride, which prevents intermolecular hydrogen bonding (Figure 8). Strong hydrogen bonding between hydroxyl groups are anticipated to reduce reactivity [46,47].

Moreover, the production of ester derivatives like cellulose acetate uses this process [38]. Acetyl reagents usually cause the cellulose fibers to expand, increasing their surface area and quickening the process. Before beginning, some authors try to "activate" the surface [44].

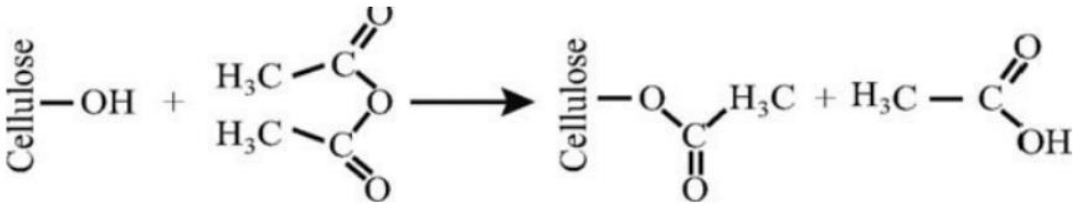

Figure 18. Acetic anhydride reaction with a primary hydroxyl group

2.3.2 Surfactants

The choice of isolation techniques has a significant impact on the surface chemistry of CNC and CNF [34]. For instance, TEMPO-meditated oxidation and sulfuric acid hydrolysis confer a negative surface charge, and the cellulose may still include anionic groups from the cell wall. Electric charges, hydration, solubility, and the type of surfactants employed all affect how well cellulose adheres to a surfactant. Although the usage of anionic surfactants such alkyl sulfates and carboxylates should be ineffectual due to the negative zeta-potentials on both opposites, some anionic surfactants have a tendency to adsorb onto negative bearing cellulose groups [34]. Anionic surfactant adsorption onto cotton is said to attain 50% saturation in 10 minutes and increase with temperature.

At the cellulose/water interfaces, it is insufficient to compete with cationic surfactants. According to [34], there are countless unexplored possibilities in the field of complex interactions.

2.4 CNF infused PLA

2.4.1 Thermal Stability

To change the thermal properties of polymers, employ nanocellulose. Free radicals and glucose are produced when the glycosidic linkages in cellulose are broken down thermally. While burning wood, cellulose is primarily responsible for the volatile chemicals that are produced [29]. The DP is constantly reduced above 200 °C to create carbonyl, carboxyl, and hydroperoxide groups [29]. Degradation is additionally increased by water, acids, and oxygen and occurs as a result of

decarboxylation, transglycosylation, and oxidation processes [29]. The temperature and rate of thermal deterioration are influenced by the physical shape and surface chemical. In an effort to compare the thermal properties, TEMPO-oxidized CNF degradation began at 300 °C in a nitrogen environment, whereas untreated CNF degradation began at 200 °C [29].

2.4.2 Characterization

There are numerous techniques that may be used to ascertain the properties of nanocelluloses. Microscopy, transmittance analysis, and rheology measurement are the best techniques for measuring its physical qualities, according to [35]. [31] Due to the fact that CNF is often held in liquid solutions, most often water, rheology testing is a frequent strategy. The concentration of cellulose in the suspensions is kept below 2 wt% to avoid clogging equipment and to make handling easier [29]. CNF suspensions exhibit gel-like properties in an aqueous phase at concentrations as low as 0.125% due to their large surface area, abundance of reactive hydroxyl groups, and increased Einstein coefficient (increasing length to diameter ratio). The viscosity rises exponentially with increasing CNF concentration [29,35].

2.4.3 Life

When managed properly, cellulose can have a longer shelf life than any other type of biomass. Aqueous solutions may be preserved for a longer period of time in the refrigerator since preservability is mostly a function of temperature. It is advised to immediately freeze goods after manufacture for even extended storage durations. Since deterioration and microbial development influence viscosity, strength, reactivity, and other CNF qualities, touching and contamination should be avoided. It is advised to utilize the material within three months of treatment for demanding applications [35].

2.4.4 Polylactic Acid

Biodegradable polymers, often known as polymers derived from biological sources, provide a viable alternative to many petrochemical polymers. They are difficult to deal with since the attributes always vary depending on the source [49].

The majority of biopolymers breakdown through biological processes into gases (CO2, N2), biomass, water, and inorganic and organic salts [49]. It is important to remember that not all bioderived polymers will biodegrade, while certain petrochemical polymers will [50]. Due to its similar properties and substantial industrial development, polylactic acid (PLA) is now commercially accessible in large quantities at competitive rates. This makes it a viable contender to replace petroleum-based polymers [41].

Produced using renewable resources including corn, sugar beet, and cassava. Starch-derived PLA was employed for this project. In the production process, it is transformed into dextrose, a kind of glucose, by hydrolysis. Lactic acid is then produced by fermentation, and following esterification, the final product in figure 10 is produced [51]. PLA hydrolyzes into acid and alcohol and is biodegradable. Temperature, moisture, and any acids and bases that are present speed up this process [52]. Polyester that is thermoplastic and aliphatic is nonpolar. Organic and inorganic fillers, nucleating agents, and other techniques are frequently employed to enhance the crystallization kinetics of biodegradable polymers due to their sluggish crystallization rate and low service temperature [43].

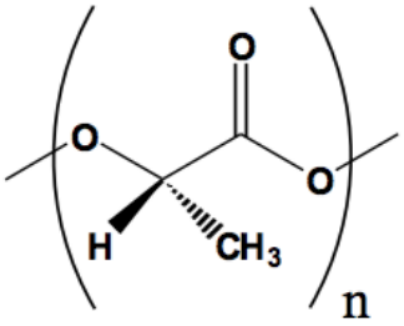

Figure 19. PLA

2.5 Application

There is a chance to use CNF in a range of applications because of the reasonably effective processing techniques made possible, allowing the generation of enormous volumes of CNF [31]. Commercial and laboratory initiatives are continuously developed with great aspirations for prospective markets. There are several large-scale, common, low-volume, and innovative uses among them, some of which are given in table 3. [53]. Due to CNF's capacity to build dense networks with superior barrier qualities, particularly high oxygen penetration resistance when compared to polymeric materials, its application in packaging has increased significantly in recent years [54].

This works well as a coating or intermediary layer in thin film applications. All uses of nanocellulose face clear difficulties, although in certain cases, strong motivation and solutions have been put up. With cellulose's capacity for self-assembly, it may be utilized on its own in a vast array of applications. The application potential of CNFs as a filler in polylactic acid is investigated in this paper. Green nanofillers are appealing due to their biodegradability as well as their low cost and strong mechanical characteristics [47].

Table 3. Applications of CNF

High volume	**Low volume**	**Novel and emerging**
Automotive	Wallboard facing	Reinforcement fibre
Cement	Insulation	Filtration and purification
Paper coatings	Aerospace	Rheology modifiers
Paper filler	Aerogels	Cosmetics
Plastic replacement	Paints	Medical applications
Hygiene products		Flexible electronics
Textiles for clothing		3D printing

2.5.1 Composite

Composites are assemblages of two or more materials having varying contents and phases [49]. In order to achieve a combination with an overall higher performance, a lower modulus, continuous

phase (matrix) is often utilized in conjunction with a dispersed reinforcing phase (filler) [49]. Three categories can be used to classify composites [55]. In the first kind, a matrix-suspended reinforcement made of particles is used. The second uses many phases that are layer by layer attached to one another and is frequently referred to as structural composites or sandwich composites. The third option is fiber reinforced composites, which make use of long fibers incorporated into a matrix. In order to change the matrix's characteristics, such as weight, electrical conductivity, strength, and even cost, a filler material is introduced on purpose.

It is essential to remember that all fillers affect the mechanical characteristics of polymeric materials [48]. Processing techniques are the primary cause of composite property variation since particle dispersion, distribution, and alignment determine the final characteristics of the material [48]. Although it is preferable for nanoparticles to be dispersed equally across nanocomposites, there are currently no known ways to regulate this behavior [45].

2.5.2 CNF used as a reinforcement

The coming generation underpinning for high performance green mixes is constantly seen as the natural structural polymer with a big face area and high strength [56] numerous ways for creating CNF and CNC on a small scale in the laboratory have redounded in a lot of papers on mixes [56]. [29] asserts that integrating traditional high- modulus mounts with a polymer matrix improves the compound's modulus and strength but decreases its total impact strength and rigidity. Using slightly dispersed nanoparticles coupled in a three- dimensional network rather of traditional mounts minimizes stress attention and increases strength without immolating rigidity and impact strength. Because CNF can form a oozed network, the strongest buttressing goods on thermoplastics have been shown at low attention of CNF. Estimates place the threshold for the needed percolation action at 1- 6 vol [56]. It seems that when abecedarian fibril cling is present in large amounts, the thick cellulose networks are less likely to be saturated by polymers [56]. A broader glass transition range and lesser strength above the glass transition temperature are farther counteraccusations for mixes made by solvent casting unaltered CNF with homogeneous dissipation [35]. As compared to glass and natural fibers, which have surface areas below 10 m^2g^{-1}, CNF has a surface area of 100–200 m^2g^{-1}, which is enormous.

2.5.3 Types of CNF reinforcements

[46] employed nanocellulose as a padding in thermoplastic polymer matrices for the first time in 1987, but it was not until [52] used cellulose microfibrils in polymer matrices in 1995 that the full buttressing impact of modest amounts came apparent [56]. After this, due to its ease of dissipation in waterless results and substantial buttressing eventuality, cellulose was employed in hydrophilic elastomers and water-answerable polymers, similar as potato bounce [56]. For these operations, water-answerable polymers may be dissolved and combined directly with an waterless cellulose result, doing down with the demand for labor- ferocious compounding, solvent exchange, and drying styles [29].

After combining the two corridor, water can be removed using evaporation, filtration, snap drying, or hot pressing. The underpinning and matrix can interact explosively since both of the rudiments are polar[48]. Another strategy to get around the dissipation issue and vastly enhance mechanical characteristics was proposed in 2005. To do this, nanopapers saturated with thermosetting polymers were created [48]. In laminated mixes, nanopapers can be employed as 2D mounts because of their predictable characteristics[38].

2.5.4 PLA/CNF composites

Avoiding flocculation is a big challenge when making PLA/CNF composites since the hydrophilic cellulose does not mix well with the hydrophobic matrix material [57]. The polar cellulose fibrils need to be modified to become more hydrophobic and enhance interfacial adherence to the matrix since they can create severe dispersion- and compatibility issues in non-polar media [42]. Long fibrils agglomerate as a result of contradictory material qualities that hinder optimal dispersion, which lowers surface area and mechanical performance. Lignocellulosic fibers often enhance PLA's tensile qualities at the expense of impact strength and brittleness. The absence of contact between the fiber and matrix can be used to explain this [39].

The CNF's affinity for water is thought to be reduced by acetylation, which also increases the CNF's compatibility with nonpolar solvents and matrices [58]. After being cleaned and solvent

swapped with the necessary solvents, the CNF is frequently subjected to a significant excess of acetic anhydride during the acetylation process in order to optimize the DS. According to [58], when the DS increased, the number of aggregates dropped and the films became more clear (Figure 11). Nonetheless, the mechanical strength of unmodified fibers was much higher than that of acetylated fibers. While measuring the DS, FTIR spectroscopy is used [58]. There have been conflicting outcomes reported when using nanocelluloses as nucleating agents. According to [41]. PLA/CNF composites have a considerably greater rate of crystallization than plain PLA. According to the CNF content in that investigation, the nucleation power also rose.

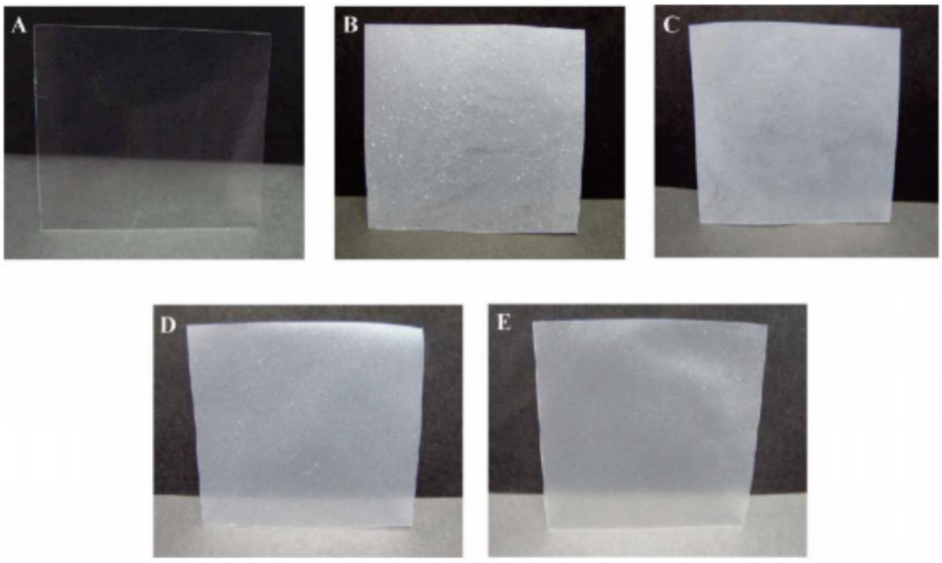

Figure 20. PLA and PLA/acetylized films produced by [58] (A) Neat PLA (B) 10 wt% unmodified CNF (C) 10 wt% acetylated CNF with DS 3,5% (D) 10 wt% acetylated CNF with DS 8,5% (E) 10 wt% acetylated CNF with DS 17% [58]

2.6 Methods

To produce a continuous nanoparticle network of single fibrils during the mixing of CNF into a matrix, sufficient dispersion is essential [29]. According to quantitative study, solution casted samples have the highest mechanical characteristics possible for a given polymeric system and the majority of solvent casting techniques allow for the maintenance of the dispersion state [29]. Particles have time to reorganize and form a network because of the Brownian motion and the

comparatively slow evaporation rate. Melt compounding with a twin screw extruder moving in the opposite direction has produced good dispersion [48]. In this section, two popular composite fabrication techniques are examined.

2.6.1 Solvent Casting

Solvents are frequently used to disperse particles in nanocomposites. either by carrying out the procedure as a solvent transfer or a solvent combination. For the purpose of suspending the particles, solvent mixes need a polymer solution with a water miscible solvent. Processing techniques include compression molding and solvent evaporation, for instance.

The CNF is transported to and suspended in a solvent during a solvent exchange procedure. This procedure also makes it possible to further surface-modify the nanoparticles by using the liquid suspension as a medium [29]. When the polymer matrix is dissolved and the solvent-borne particles are added directly into the polymer solution, a suspension with a higher particle dispersion is produced than when the particles are added to a polymer melt [36]. A flat surface, like a glass plate or a PTFE mold cleaned with acetone, should be utilized for casting. Release coatings should not be used, according to [59] since this might produce artifacts during the analysis step. The solvent is evaporated after adding the polymer solution to the mold. Depending on the evaporation rate, the appearance and texture of composites made through solvent casting might vary [59].

This approach has been employed in laboratory-scale manufacturing to achieve acceptable dispersion in place of a dry compounding stage. In order to create PLA/microcrystalline cellulose filament, [57] solvent cast films, ground them, and then used a twin-screw extruder to extrude them. In this instance, processing temperatures between 165 and 190 °C were chosen in the hopes that the cellulose wouldn't degrade due to heat. The glass transition range was broader and the strength was greater in the 3 and 5 wt% CNF/PLA films with both natural and modified fibers.

2.6.2 Melt compounding

Melt processing is crucial to the sector since it is easy, affordable, and scalable. The melts can be treated either in batches or continuously, depending on the manufacturing size [41]. Microextruders are recommended for pilot projects and laboratory scale activities [48]. It is important to remember that microextruders have lengthy processing durations, which frequently cause cellulose or the matrix polymer to degrade. In the extrusion process, the nanocellulose can be added to the polymer melt either in dry form or as a liquid suspension, each of which has conceptual benefits and disadvantages. The fact that extruders frequently function as closed systems traps the steam and gas produced by the frequently aqueous nanocellulose suspensions.

Due to the intricacy of energy-intensive and time-consuming drying procedures, solution feeding is more economical. Also, depending on changes made to its surface chemistry, dry fluffy fibrils might be challenging to redisperse [41].

2.7 Characterization and Testing

Testing of materials is done to categorize their characteristics and performance. Different characteristics of materials may be determined using a variety of techniques, and research and development are supported by the quantitative data collected. In this section, some crucial techniques for analyzing nanocomposites are covered.

2.7.1 FTIR Spectroscopy

There are several systems that may be used to detect polymers and reactions, and spectroscopy examines the interactions between radiation and materials. FTIR, sometimes referred to as infrared spectroscopy, manipulates molecules' vibration and rotation by using electromagnetic radiation in the infrared area. These distinguishing vibrations aid in determining the chemical composition of additives and polymers [60].

2.7.2 DSC

The thermal transition times of polymers may be found via differential scanning calorimetry. This compares the heat needed to raise the temperature of a polymeric sample to a reference object that does not react in the necessary testing range and has transitional times that are precisely defined. Tin and mercury are frequently employed as the reference objects [48]. The operating range for many DSC equipment is in the milligram range (10 mg).

2.7.3 Mechanical Testing

The mechanical behavior of materials at various temperatures may be tested using dynamic mechanical analysis (DMA) (Dufresne, 2018). This enables the user to research the effects of reinforcements outside the matrices glass transition range. A tensile testing equipment is used to characterize the tensile characteristics of the material (ASTM International, 2002). Results vary depending on sample size, processing methods, testing speed, grips employed, and extension measurement method. Results from tensile tests offer information for quality and specification requirements, as well as for research and development. A tensile testing apparatus consists of various parts. Rubber-lined grips with one linked to a moveable part that hold the sample. a drive system that moves the moveable part at a user-configurable constant speed. a load indicator that displays the tensile force placed on the object the moving grips are holding. With the values collected, the ultimate tensile strength may be determined by:

UTS = F/A

Where F is the greatest force applied, A is the nominal cross-sectional area of the specimen, and UTS is the ultimate tensile strength. The following formula is used to compute standard deviation (ASTM International, 2002):

$$s = \sqrt{\frac{(\sum X^2 - x)}{n - 1}}$$

Where n is the number of observations, X is the value of one observation, and x represents the mean of the collection of data.

2.7.4 Microscopy

Due of its simplicity and low cost, optical microscopy is frequently used to examine polymers [59]. With the use of polarized microscopy, flaws and the completeness of mixing may be observed; this is especially useful for fiber-reinforced semicrystalline polymers where the components can be easily separated. The size distribution of the particles in CNFs should be less than the visible range.

2.7.5 SEM

An effective technique for examining the surface topography of polymers is scanning electron microscopy [59]. The samples are grounded and placed on a conductive substrate. Non-conductive samples need to be coated to reduce charging since negative charges might build up on the sample surface, which will result in bright spots on the picture.

3. EXPERIMENTAL WORK

3.1 Introduction

Using acetylated and unmodified CNF, the goal of this experimental effort was to create 3D printed PLA/CNF composites with a CNF concentration of 1, 3, and 5 wt%. A clean PLA film should also be produced for reference. It was intended to compare the tensile strength of composites made of acetylated and untreated fibrils to that of neat PLA. This thesis involved the creation of several samples, and through trial and error, the procedure was improved.

Due to its potential for direct digital production and additive manufacturing, fused deposition modelling (FDM) 3D printing is a growing industry in a range of industries, including automotive and medical engineering [1-4]. 3D printing has already started to be used in the aerospace and automobile sectors to create interiors, fittings, and accessories [5]. This is due to the fact that 3D printing has special advantages including customizable design options, increased mechanical effectiveness, and the capacity to build accessories with more adaptability [6, 7]. Unfortunately, there are currently few instances of 3D printed aircraft and automobile parts made from eco-friendly materials. Traditional fiber and fabric production processes sometimes use potentially harmful or physiologically changing compounds, which has negative effects on the environment.

Moreover, there are still problems with post-consumer component recycling's efficiency and cost [9,10]. Emerging fabrication technologies, like 3D printing, must embrace more eco-friendly processes and materials in order to meet these difficulties.

Recycled 3D printed materials are a relatively new area [11]. Yet it's anticipated that the usage of biocomposite materials in 3D printing will significantly affect the manufacturing of bio-based materials for consumer goods [2]. Polylactic acid (PLA), which is commonly obtained from maize starch and sugar cane, is one of the finest thermoplastic alternatives for biomaterials, which are frequently created from agricultural or forestry waste.

Yet, as 3D printing technology advances and penetrates new markets like the automobile and aerospace sectors, its present constraints must be resolved. In order to improve the PLA matrix's physical and chemical characteristics for 3D printing, various research have begun integrating biomass raw materials [12,13]. Nanocellulose, a product of organic cellulose, is one such substance that has been researched for its potential to strengthen PLA. Because of its low density, very fine structure, and great strength, nanocellulose is attractive [14]. It has been found to increase the crystallinity, mechanical characteristics, and degradability of the PLA matrix [15]. Nanoparticles might improve functionality, provide designers more control over material qualities, and enable custom geometries to fulfill unique product requirements [16].Micro-nanocellulose was created by Wang et al. [17] using a colloid mill and combined with the PLA matrix to create a composite filament with improved tensile strength. The manufacturing procedure, which might be chemical or mechanical, affects the creation of nanocellulose differently [18,19,20]. Low mechanical stability of nanocellulose generated by intense sulfuric acid hydrolysis is caused by sulfate half ester groups [21]. Long fibers can also be homogenized under high pressure to make nanocellulose, although this method has a significant energy cost and a risk of clogging and discharge failure.

Similar difficulties also apply to the PLA/cellulose nanofibrils (CNF) composite 3D printing technique. The homogeneous distribution of nanocellulose inside the PLA matrix is a significant issue impacting the printability and physical characteristics of the composite filament and 3D printed components [22]. In order to overcome this problem, CNF was injected into PLA in this work by mixing CNF with acetone and chloroform. The resultant CNF was vacuum dried at 60 C in an oven, and melt-extrusion was used to produce the PLA/CNF composite filaments.

It was investigated and compared to standard PLA, which was utilized as a control, how the mechanical behavior of the 3D printed components behaved. Melt-extruded 3D printed PLA/CNF composite specimens were subjected to tensile, flexural, and compression testing. The results of the tests were examined to determine the performance of the composite material. According to the study's findings, adding CNF greatly enhanced the mechanical qualities of the 3D-printed components when compared to the PLA-only control samples. The PLA/CNF composites were found to have better tensile strength, flexural strength, and compression strength, indicating that they could tolerate more stress and strain.

In this study, a thorough analysis of the mechanical behavior of 3D-printed components made of polylactic acid (PLA) filaments infused with cellulose nanofiber (CNF) was conducted. This study's goal was to create PLA filaments with CNF infusions for use in 3D printing by using CNF as the reinforcing filler and PLA pellets as the matrix material. Tensile, flexural, and compression tests of the melt extruded 3D printed PLA/CNF composite specimens were carefully carried out to evaluate their mechanical characteristics. The outcomes of these tests were then contrasted with those of control samples made from ordinary PLA using 3D printing.

3.2 Methodology

3.2.1 Materials

In this investigation, pellet-sized polylactic acid (PLA) was added to cellulose nanofibrils (CNF), which were purchased commercially from Nanografi, Turkey. The PLA utilized in this investigation was likewise obtained commercially from Natureworks LLC. It had a density of 1.26 g/cm3, a melt flow index that ranged from 4 to 8 g/10min, an average molecular weight of 120,000 g/mol, a glass transition temperature of 51 °C, and a melting point of 150 °C. Acetone and chloroform were added to the PLA pellets in a 9:1 ratio, respectively, to create the CNF infusion.

3.2.2 Processing

The three-step technique for creating the nanocomposites included the following steps: (1) creating a master batch using a solvent mixture; (2) melting the filament; and (3) 3D printing components utilizing the resultant melt extruded filaments.

Table 4. Masterbatch composition

Materials	Master batch			Bulk PLA (g)	Final composition (%)
	PLA (g)	CNF (g)	Solvent mixture (g)*		
PLA	15	-	300	85	PLA (100)
PLA-CNF1	14	1	300	85	PLA-CNF (99\1)
PLA-CNF3	12	3	300	85	PLA-CNF (97\3)
PLA-CNF5	10	5	300	85	PLA-CNF (95\5)

3.2.3 Preparation of Masterbatch

Three critical processes were involved in creating the nanocomposites. The masterbatch preparation was the initial stage, which entailed combining the necessary quantity of polylactic acid (PLA) with acetone and chloroform in a 9:1 solvent ratio. To guarantee homogeneity, the dissolution was carried out at 60°C with constant stirring. When the PLA had completely dissolved, CNF was added by switching the CNF suspension's aqueous medium's solvent to an acetone-chloroform solution. A succession of centrifugation and re-dispersion procedures were used to achieve this. The final composite mixture was then poured onto Petri dishes and allowed to evaporate at room temperature for a day before being vacuum-dried for eight hours in an oven at 60°C.

The last stage entailed using a household blender to grind the composite films created during the casting process into a particle substance. The melt extrusion process's initial material was this particle substance. Table 1 is a list of the various PLA and CNF combinations' compositions. In order to achieve appropriate CNF dispersion within the PLA matrix, it is necessary to highlight that the masterbatch preparation procedure is essential. Inadequate CNF dispersion might lead to non-uniform distribution of the nanofiber and adversely affect the mechanical characteristics of the finished composite. The CNF is effectively dissolved and homogenized inside the PLA matrix thanks to the dispersant's usage of an acetone and chloroform solvent combination. To create a particle material appropriate for the melt extrusion process, further drying and crushing stages were required.

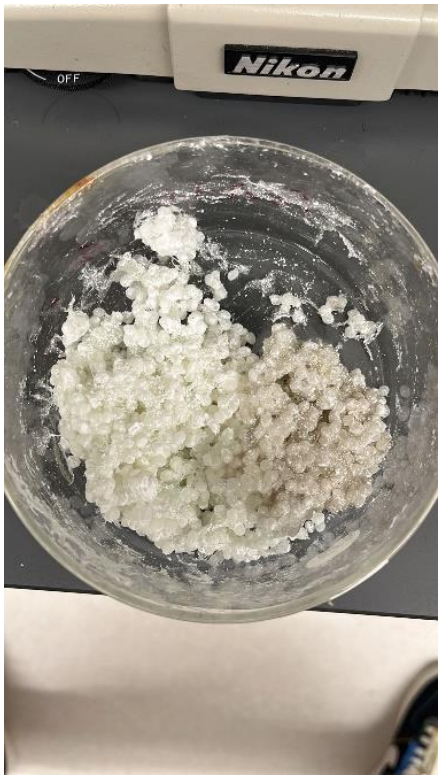

Figure 21. PLA/CNF masterbatch

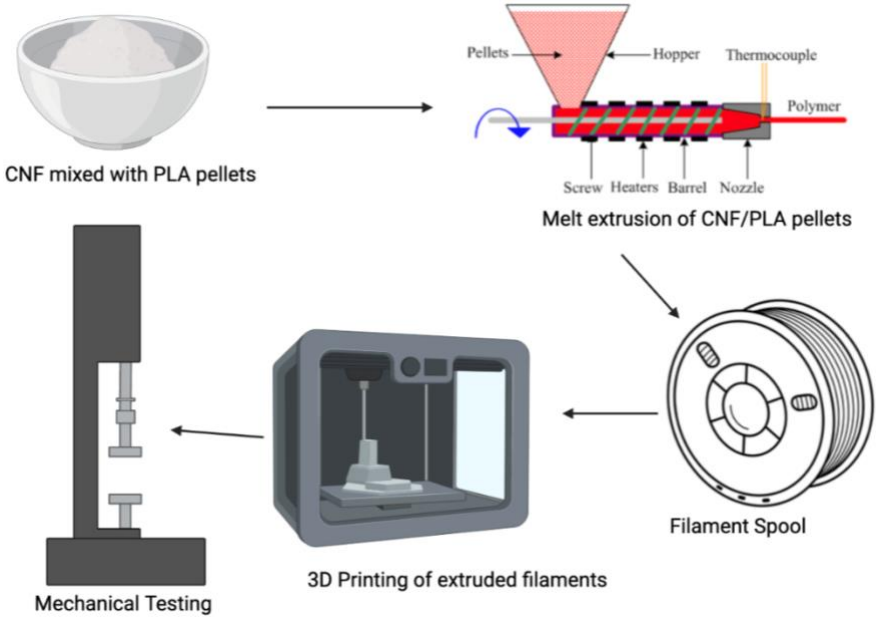

Figure 22. Manufacturing of PLA/CNF composite

3.3 Melt Extrusion

Using a Filabot EX2 melt extruder, the nanocomposite filaments for 3D printing were created. The temperature profile was tuned to vary from 170°C in the feeding zone to 190°C at the die, and the screw speed was set at 120 revolutions per minute. At weight percent concentrations of 1%, 3%, and 5% nanofiber, the master batch was crushed and uniformly combined with the PLA. Prior to being used in 3D printing, the compounded PLA and its corresponding nanocomposites underwent an 8-hour vacuum drying procedure at 60°C.

Figure 22 (a) illustrates the melt-extruded nano-composite filaments gathered on a spool attached to a Filabot Spooler-Precision Filament Winder with a diameter of 1.75mm. Figure 22 (b) shows the filament extrusions produced.

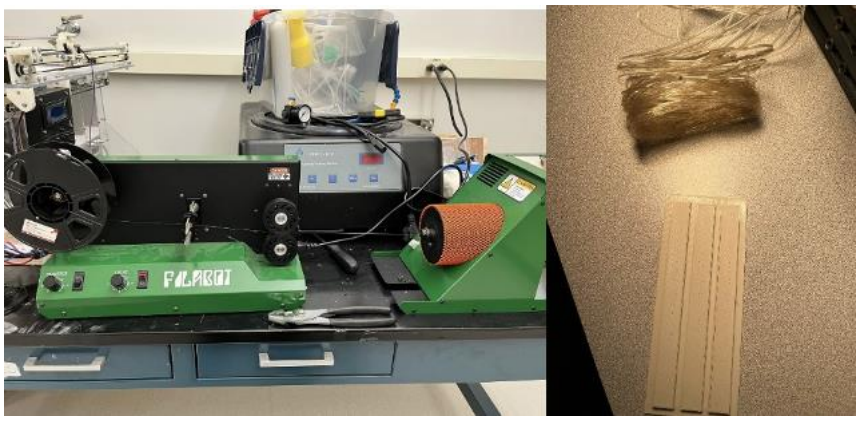

Figure 23 (a) Melt extrusion of PLA/CNF masterbatch, (b) Filament used for 3D printing mechanical test specimens.

3.4 3D Printing and Mechanical testing

Three-dimensional (3D) printing was used to create assessment prototypes using the created filaments. The Ultimaker 3 FDM desktop 3D printer and Ultimaker Cura slicing program were used to turn the computer-aided design (CAD) models into actual things. A 0.4mm nozzle was used during the 3D printing process, and the extruder temperature was set at 210°C with a printing speed of 50mm/s. Simple specimens were created in line with ASTM standards as illustrated in Figure 22 to examine the mechanical characteristics. The normal PLA samples and the CNF/PLA

nanocomposites (1, 3, and 5wt%) were next subjected to mechanical testing, which included tensile, flexural, and compression tests, as shown in Figure 23.

Figure 24. Flexural test specimen

3.5 SEM

By breaking the films under cryogenic conditions in liquid nitrogen, representative cross-sections were produced. The sliced and shattered samples were taped on an aluminum stub with conductive double-sided carbon tape. To guarantee that all samples were grounded in the vertical plane, hand-painted colloidal graphite was applied. Using a Cressington sputter coater 210 HR, a 10 nm thick coating of Au/Pd alloy was then sputter coated onto the stub after being flushed with argon.

4. RESULTS AND DISCUSSION

4.1 Morphological observation

The polylactic acid (PLA) matrix was infused with the commercially obtained cellulose nanofiber (CNF). The purpose of the morphological investigation was to determine whether CNF agglomerations were present on the cracked surfaces. The pictures using scanning electron microscopy (SEM) revealed that the pure PLA had a smooth surface with typical brittle fracture characteristics. Nevertheless, the 1wt% CNF/PLA composite's mechanical strength was not greatly increased because there was not enough CNF present to create strong interfacial connections with the PLA matrix. The 3wt% CNF/PLA composite's excellent tensile properties can be attributed to the CNF's extensive mixing with the PLA matrix. Some fiber breakages were seen on the composite's fractured surface, but there was no sign of an agglomeration.

The apparent aggregation shown in the SEM pictures of the 5wt% CNF/PLA composite may have resulted from a loss of compatibility between the PLA and high CNF concentrations. The aggregation of the CNF is what causes the PLA/CNF nanocomposites' tensile strength to diminish with increased CNF loading (beyond 3 wt%). Poor interfacial adhesion between the CNF and PLA was caused by the CNF fibers' tendency to aggregate and form bigger clusters as the CNF loading increased rather than connecting with the PLA matrix.

Raman Spectroscopy

Raman spectroscopy of unadulterated PLA and PLA-CNF composites is illustrated in the figure 25. The pristine PLA spectra are characterized by stretching C=O groups at multiple wavenumbers. Weak C=O groups are observed within the frequency range of 680 cm^{-1} to 750 cm^{-1}, whereas moderate groups are located between 740 cm^{-1} and 775 cm^{-1}. Strong C=O groups in the PLA polymer manifest within the frequency range of 1750 cm^{-1}, 1653 cm^{-1}, and 1780 cm^{-1}. C=O groups exhibit broadening within the 1710 to 1810 cm^{-1} frequency range. Notably, the stereo complex, commonly observed at 1755 cm^{-1}, is absent. A specific peak group in the PLA polymer, representing asymmetric CH groups, appears at 1465 cm^{-1}. In contrast, the

deformation asymmetric CH_3 group of PLA shifts to a wavenumber of 1410 cm^{-1}. The functional CH_3 symmetric group, typically emerging within the 1386 to 1390 cm^{-1} frequency range, shifts to 1390 cm^{-1}. CH_3 asymmetric groups, usually detected at 1130 cm^{-1}, remain stable at 1128 cm^{-1}. Raman spectra within frequency ranges of 1182 and 1218 cm^{-1} correspond to moderate C-OC asymmetric groups and very strong C-O-C symmetric groups at a wavenumber of 1105 cm^{-1}. Upon the integration of CNF networks into PLA resin, the Raman band initially positioned at 1097 cm^{-1}, deriving from cellulose, can be identified in the composites. PLA films show a minor peak near the 1097 cm-1 peak, but the intensity is insufficient to interfere with the cellulose signal. This peak is visible in the pure resin material but becomes less visible when cellulose is combined with PLA. Concerning the tensile strain of neat PLA films, no shift in the PLA peak proximal to the cellulose peak is observed. This observation implies that the previously documented shift in the position of the Raman band initially at 1097 cm1 obtained from CNF-reinforced composites is not influenced by the band in the identical region emerging from the PLA resin. The absence of this shift is thought to be due to the entangled network of polymer molecules in PLA, which lacks any preferential orientation.

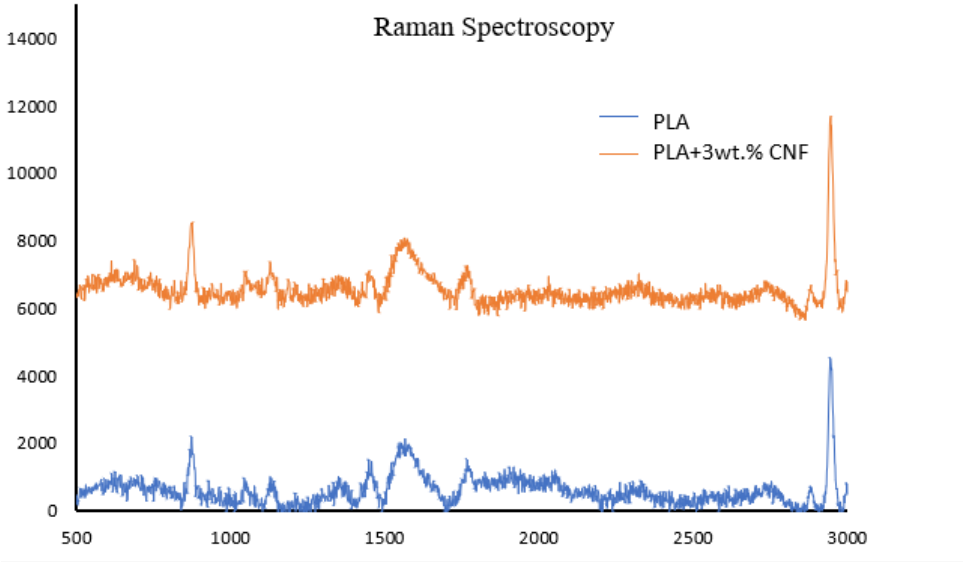

Figure 25. Raman spectroscopy

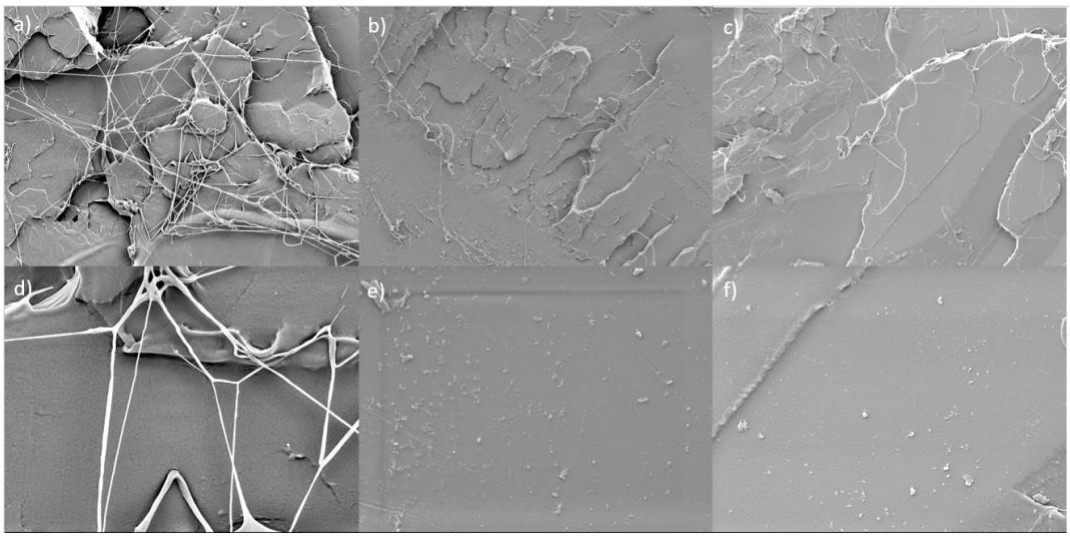

Figure 26. (a,d) SEM micrographs of cross-section of 3wt% PLA/CNF; (b,e) PLA/CNF 1 wt.%; (c,f) PLA/CNF 5 wt.%; scale bar=10nm

4.2 Tensile Test

In line with ASTM D638/ISO 527-2 standards, the mechanical qualities of melt-extruded CNF/PLA filaments were assessed by tensile testing utilizing a Universal testing machine on 3D printed dog bones using an FDM (Fused Deposition Modeling) 3D printer (Ultimaker 3). Figure 1.4 shows the observed tensile strength and elongation at break of the PLA/CNF filaments. Because of the increased interfacial adhesion between the CNF and PLA, the addition of CNF increased the tensile strength and elongation at break of the PLA filaments. At a tensile strength of 85.86 MPa and a 3wt% loading, the best mechanical stability was found. The equally dispersed CNF inside the PLA matrix created by the addition of solvents like chloroform and acetone, which led to the creation of hydrogen bonds between the CNF and PLA, is responsible for the increase in mechanical characteristics. As seen by the average tensile strength of 79.33 MPa for the 5wt% CNF composite, larger CNF loadings than 3wt% can partially aggregate inside the PLA matrix, resulting in a reduction in tensile strength and deterioration of the composite material's mechanical characteristics. SEM (Scanning Electron Microscopy) was used to analyze the cross-sectional characteristics of the specimens, and it was found that, in contrast to the smooth surface of the pure PLA, the cross-section of the specimens became progressively uneven and fibrous with increasing CNF concentrations.

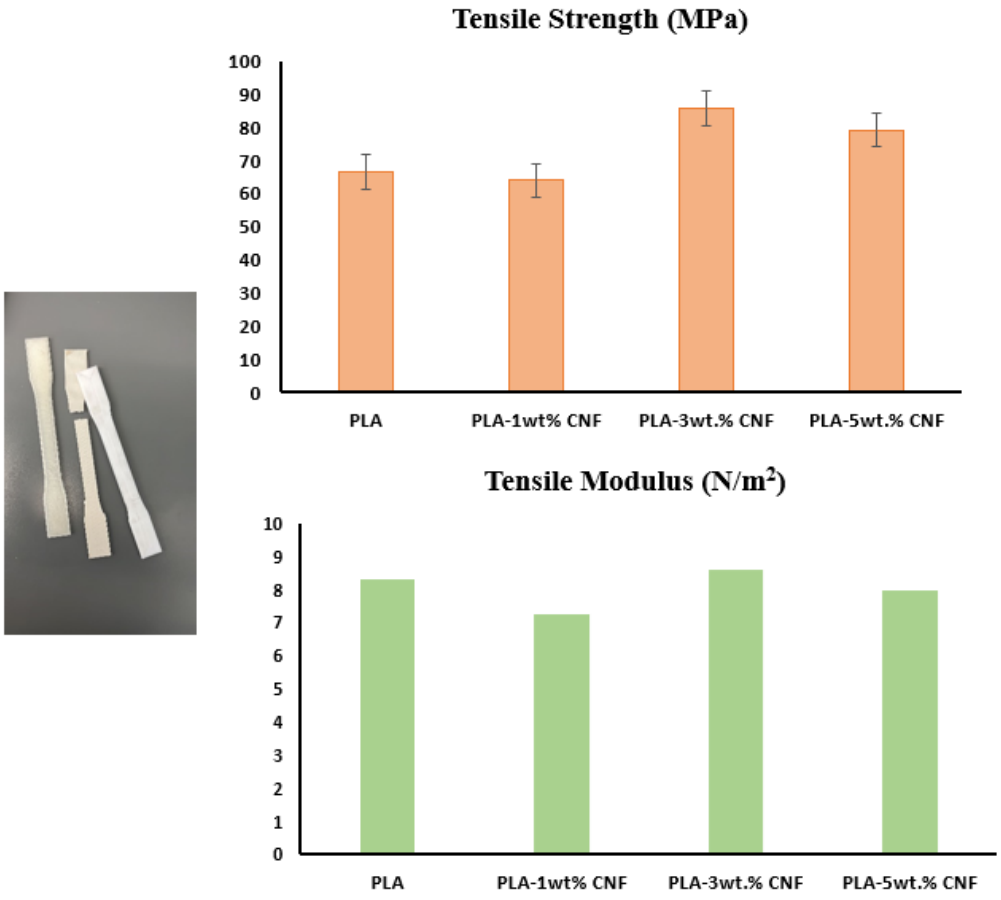

Figure 27. Tensile Strength and Modulus

4.3 Compression test

Using a Solidworks model and an Ultimaker 3 printer, 3D printed cylinders with a 70% infill rate were created in order to assess the impact of cellulose nanofibrils (CNF) on the compressive characteristics of polylactic acid (PLA) composites. Twelve of each type of sample—prinstine PLA, CNF/PLA1, CNF/PLA3, and CNF/PLA5—were created for the experiment and fabricated in accordance with ASTM D695 standards. A compression test was then performed on the samples using a universal testing machine. As compared to pure PLA, the composites' compressive yield strength significantly increased, according to the data. The average compressive yield strength of the CNF/PLA3 samples was 104.93 MPa, while the yield strength of the pure PLA was 65.8 MPa.

The yield strength measurements for the CNF/PLA1 and pure PLA samples were 71 MPa and 65.8 MPa, respectively. The CNF/PLA5 sample, with an average compressive strength of 80 MPa, however, showed a considerable reduction in compressive strength. Regardless of the CNF loading, it was discovered that voids and a lack of interfacial bonding were the significant contributors to the yield strength distribution. In this investigation, it was shown that adding 3 wt% CNF to the composite greatly increased its compressive strength, however adding more CNF than this had the opposite effect. Figure 27 shows the outcomes of the compression testing.

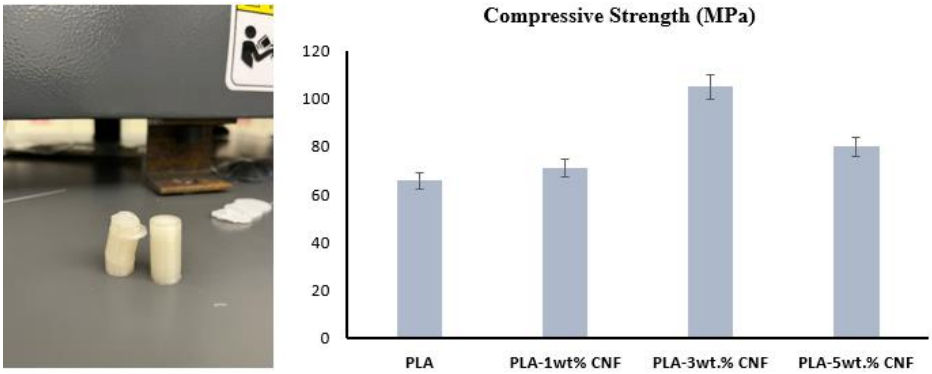

Figure 28. (a)Typical Compression test specimen before and after test (b)Compressive Strength

4.4 Flexural Test

According to ASTM D790 specifications, the Flexural specimens were created utilizing Fused Deposition Modeling (FDM) 3D Printing technology and the Ultimaker 3 machine. For the aim of performing experimental testing, a total of 12 specimens of both pure Polylactic Acid (PLA) and PLA that had been infused with Carbon Nanofiber (CNF) were produced. In order to assess the samples' flexural properties, a three-point bending test was carried out using an infill rate of 70%. When tested flat-wise on a support span with a minimum radius of 3.2mm, as illustrated in Figure, the specimens of thermoplastics and thermosets are required to have a length of 12.7mm and a height of 3.2mm, according to ASTM D 790 requirements.

As the sample was made with a popular 3D CAD program, it was transmitted in the.STL file format, which is utilized for 3D printing. A rectangular specimen with dimensions of 13.8mm (b), 13.5mm (h), and 3.5mm underwent a three-point bending test (h). The specimen was placed

between two supports that were 100 cm apart, as shown in Figure, and a force was applied by an actuator at the precise center of the two supports (L/2). The maximum flexural strength (s) and Young's modulus (E) of the specimen were determined by computing the load vs. displacement curve. The elastic modulus was calculated using the slope of the stress-strain curve's straight-line segment. The outcomes are displayed in the figure below.

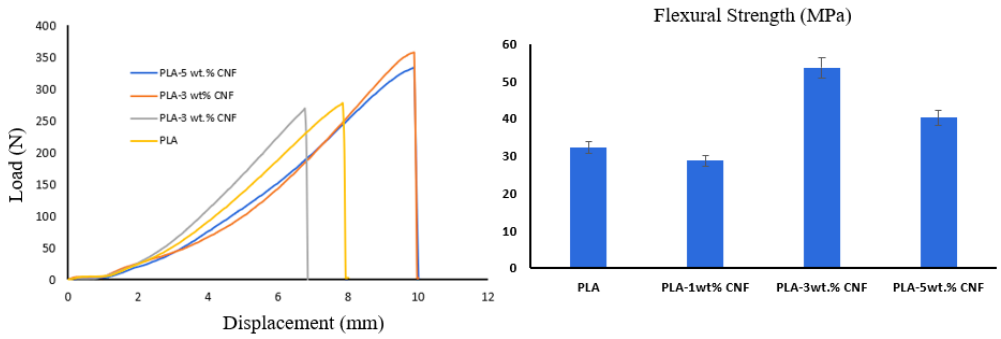

Figure 29. Flexural test

Based on weight %, the flexural performance of polylactic acid (PLA) and PLA packed with carbon nanofiber (CNF) was compared and assessed. According to the findings, the pure PLA had a maximum flexural strength of 32.3 MPa. The 3wt% CNF loaded PLA had the greatest flexural strength, measuring 53.65 MPa, a 60.2% improvement over the pure PLA. As compared to pure PLA, the flexural strength of the 1 and 5wt% CNF loaded PLA specimens was reduced. According to the findings, 3wt% of CNF is the ideal weight percentage for increasing PLA's flexural strength. The 1 and 5wt% CNF loaded PLA specimens showed a greater Young's modulus value compared to the pure PLA.

The PLA filled with 1 and 5wt% CNF had the greatest Young's modulus value, measuring 18.5 GPa. The 3wt% CNF loaded PLA has a Young's modulus of 16.3 GPa compared to the pure PLA's 17.62 GPa. These findings imply that 1 or 5wt% CNF is the ideal weight percentage for increasing the Young's modulus of PLA.

5. CONCLUSION

In this work, cellulose nanocomposites (CNF) were synthesized utilizing a master batch that had a significant amount of nanofibers in polylactic acid (PLA). Extrusion was used to combine the master batch with the bulk PLA to create nanocomposites with various fiber compositions. Microscopical research revealed that the PLA-CNF3 nanocomposite did not display any substantial CNF agglomeration when the fracture surfaces of the nanocomposites were examined morphologically. Minor aggregation was seen in the PLA-CNF5 composite, proving that the nanofibers were not evenly distributed throughout the material. Little white spots were visible after additional visual examination of the materials generated, especially in the composites containing 5 wt% CNF, which further supported the aggregation of nanofibers. It was discovered that the composites developed a less securely cross-linked structure with no bonding when the CNF weight percentage was low (1 wt%). A trend was noticed in the mechanical characteristics of the PLA and its nanocomposites, where the tensile strength and modulus rose with increasing nanofiber content. The tensile strength of the composite rose from 66.72 MPa to 85.86 MPa when 3 wt% nanofibers were added to the PLA, while the tensile modulus increased from 8.3 N/m^2 to 8.58 N/m^2. Moreover, the flexural strength increased by 60.2% while the compressive strength increased by 62.7%.

REFERENCES

1. Wang Q.Q., Sun J.Z., Yao Q., Ji C.C., Liu J., Zhu Q.Q. 3D printing with cellulose materials. Cellulose. 2018;25:4275–4301. doi: 10.1007/s10570-018-1888-y. [CrossRef] [Google Scholar]
2. Liu J., Sun L., Xu W., Wang Q., Yu S., Sun J. Current advances and future perspectives of 3D printing natural-derived biopolymers. Carbohydr. Polym. 2019;207:297–316. doi: 10.1016/j.carbpol.2018.11.077. [PubMed] [CrossRef] [Google Scholar]
3. Wong K.V., Hernandez A. A review of additive manufacturing. Int. Sch. Res. Not. 2012;2012:208760. doi: 10.5402/2012/208760. [CrossRef] [Google Scholar]
4. Horn T.J., Harrysson O.L. Overview of current additive manufacturing technologies and selected applications. Sci. Prog. 2012;95:255–282. doi: 10.3184/003685012X13420984463047. [PubMed] [CrossRef] [Google Scholar]
5. Wellbrock, W., Ludin, D., Röhrle, L. et al. Sustainability in the automotive industry, importance of and impact on automobile interior – insights from an empirical survey. Int J Corporate Soc Responsibility 5, 10 (2020). https://doi.org/10.1186/s40991-020-00057-z
6. Lecklider, Tom. "3D printing drives automotive innovation." EE-Evaluation Engineering, vol. 56, no. 1, Jan. 2017, pp. 16+. Gale Academic OneFile, link.gale.com/apps/doc/A477460305/AONE?u=ind23893_ttda&sid=googleScholar&xid=f1919288. Accessed 26 Oct. 2022.
7. Henry A. Colorado, Elkin I. Gutiérrez Velásquez, Sergio Neves Monteiro, Sustainability of additive manufacturing: the circular economy of materials and environmental perspectives, Journal of Materials Research and Technology, Volume 9, Issue 4, 2020, Pages 8221-8234, ISSN 2238-7854, https://doi.org/10.1016/j.jmrt.2020.04.062.
8. Jackson B, Fouladi K, Eslami B. Multi-Parameter Optimization of 3D Printing Condition for Enhanced Quality and Strength. Polymers (Basel). 2022 Apr 13;14(8):1586. doi: 10.3390/polym14081586. PMID: 35458336; PMCID: PMC9030841.
9. Tanney D., Meisel N.A., Moore J. Investigating Material Degradation through the Recycling of PLA in Additively Manufactured Parts; Proceedings of the 28th Annual International Solid Freeform Fabrication Symposium; Austin, TX, USA. 7–9 August 2017; pp. 519–531. [Google Scholar]
10. Lanzotti A., Martorelli M., Maietta S., Gerbino S., Penta F., Gloria A. A comparison between mechanical properties of specimens 3D printed with pristine and recycled PLA. Procedia Cirp. 2019;79:143–146. doi: 10.1016/j.procir.2019.02.030. [CrossRef] [Google Scholar]
11. Anderson I. Mechanical properties of specimens 3D printed with pristine and recycled polylactic acid. 3d Print. Addit. Manuf. 2017;4:110–115. doi: 10.1089/3dp.2016.0054. [CrossRef] [Google Scholar]

12. Murphy C.A., Collins M.N. Microcrystalline cellulose reinforced polylactic acid bio composite filaments for 3D printing. Polym. Compos. 2018;39:1311–1320. doi: 10.1002/pc.24069. [CrossRef] [Google Scholar]

13. Mathew A.P., Oksman K., Sain M. Mechanical properties of biodegradable composites from poly lactic acid (PLA) and microcrystalline cellulose (MCC) J. Appl. Polym. Sci. 2005;97:2014–2025. doi: 10.1002/app.21779. [CrossRef] [Google Scholar]

14. Lendvai L., Karger-Kocsis J., Kmetty Á., Drakopoulos S.X. Production and characterization of micro fibrillated cellulose-reinforced thermoplastic starch composites. J. Appl. Polym. Sci. 2016;133:42397. doi: 10.1002/app.42397. [CrossRef] [Google Scholar]

15. Suryanegara L., Nakagaito A.N., Yano H. The effect of crystallization of PLA on the thermal and mechanical properties of micro fibrillated cellulose-reinforced PLA composites. Compos. Sci. Technol. 2009;69:1187–1192. doi: 10.1016/j.compscitech.2009.02.022. [CrossRef] [Google Scholar]

16. Campbell T.A., Ivanova O.S. 3D printing of multifunctional nanocomposites. Nano Today. 2013;8:119–120. doi: 10.1016/j.nantod.2012.12.002. [CrossRef] [Google Scholar]

17. Wang Z., Xu J., Lu Y., Hu L., Fan Y., Ma J., Zhou X. Preparation of 3D printable micro/nanocellulose-polylactic acid (MNC/PLA) composite wire rods with high MNC constitution. Ind. Crop. Prod. 2017;109:889–896. doi: 10.1016/j.indcrop.2017.09.061. [CrossRef] [Google Scholar]

18. Wang Q., Wei W., Chang F., Sun J., Xie S., Zhu Q. Controlling the Size and Film Strength of Individualized Cellulose Nanofibrils Prepared by Combined Enzymatic Pretreatment and High Pressure Micro fluidization. BioResources. 2016;11:2536–2547. doi: 10.15376/biores.11.1.2536-2547. [CrossRef] [Google Scholar]

19. Wang Q., Zhao X., Zhu J.Y. Kinetics of Strong Acid Hydrolysis of a Bleached Kraft Pulp for Producing Cellulose Nanocrystals (CNCs) Ind. Eng. Chem. Res. 2014;53:11007–11014. doi: 10.1021/ie501672m. [CrossRef] [Google Scholar]

20. Wang Q.Q., Zhu J.Y., Gleisner R., Kuster T.A., Baxa U., McNeil S.E. Morphological development of cellulose fibrils of a bleached eucalyptus pulp by mechanical fibrillation. Cellulose. 2012;19:1631–1643. doi: 10.1007/s10570-012-9745-x. [CrossRef] [Google Scholar]

21. Lim H, Hoag SW. Plasticizer effects on physical-mechanical properties of solvent cast Soluplus® films. AAPS PharmSciTech. 2013 Sep;14(3):903-10. doi: 10.1208/s12249-013-9971-z. Epub 2013 May 21. PMID: 23689959; PMCID: PMC3755169.

22. Mokhena T., Sefadi J., Sadiku E., John M., Mochane M., Mtibe A. Thermoplastic processing of PLA/cellulose nanomaterials composites. Polymers. 2018;10:1363. doi: 10.3390/polym10121363. [PMC free article] [PubMed] [CrossRef] [Google Scholar]

23. Wickramasinghe, S.; Do, T.; Tran, P. FDM-Based 3D printing of polymer and associated composite: A review on mechanical properties, defects and treatments. Polymers 2020, 12, 1529. [Google Scholar] [CrossRef]

24. Burg, K.J.L.; Holder, W.D.; Culberson, C.R.; Beiler, R.J.; Greene, K.G.; Loebsack, A.B.; Roland, W.D.; Mooney, D.J.; Halberstadt, C.R. Parameters affecting cellular adhesion to polylactide films. J. Biomater. Sci. Polym. Ed. 1999, 10, 147–161. [Google Scholar] [CrossRef] [PubMed]

25. Heinze, T. 2016, "Cellulose: Structure and Properties", Advances in Polymer Science, vol. 271, pp. 1.

26. Ng, H., Sin, L.T., Tee, T., Bee, S., Hui, D., Low, C. & Rahman, A.R. 2015, "Extraction of cellulose

27. Räisänen, T. & Athanassiadis, D. 2013, "Basic chemical composition of the biomass components of Pine, Spruce and Birch", .

28. Klemm, P.D.D., Schmauder, P.D.H. & Heinze, P.D.T. 2015, "Cellulose" in Biopolymers Wiley, pp. 275.

29. Dufresne, A. 2018, Nanocellulose : From Nature to High Performance Tailored Materials, 2nd edn, Walter de Gryter Gmbh, Berlin/Boston.

30. Granström, M. 2009, Cellulose Derivatives: Synthesis, Properties and Applications, University of Helsinki.

31. Rissanen, V. 2016, Process Optimization of Cellulose Fibril – The Effect of Process Medium Composition on Energy Efficiency and Product Quality, Aalto University.

32. European Commission 22/02/2017-last update, Definition of a nanomaterial. Available: http://ec.europa.eu/environment/chemicals/nanotech/faq/definition_en.htm29/04/201 8].

33. Zimmermann, M., Borsoi, C., Lavoratti, A., Zanini, M., Zattera, A.J. & Santana, R.M. 2016, "Drying techniques applied to cellulose nanofibers", Reinforced plastics & composites, vol. 35, no. 8, pp. 682.

34. Tardy, B.L., Yokota, S., Ago, M., Xiang, W., Kondo, T., Bordes, R. & Rojas, O.J. 2017, "Nanocellulose–surfactant interactions", Current Opinion in Colloid & Interface Science, no. 29, pp. 57.

35. Kargarzadeh, H., Ionelovich, M., Ahmad, I., Thomas, S. & Dufresne, A. 2017, "Methods for Extraction of Nanocellulose from Various Sources" in Handbook of Nanocellulose and Cellulose Nanocomposites, eds. Kargarzadeh, Hanieh, Ahmad, Ishak, S. Thomas & A. Dufresne, First Edition edn, Wiley-VCH Verlag GmbH & Co. KGaA., pp. 1.

36. Naderi, Ali. "Nanofibrillated cellulose: properties reinvestigated." *Cellulose* 24.5 (2017): 1933-1945.

37. Österberg, M., Vartiainen, J., Lucenius, J., Hippi, U., Seppälä, J., Serimaa, R. & Laine, J. 2013, "A Fast Method to Produce Strong NFC Films as a Platform for Barrier and Functional Materials", Applied Materials & Interfaces.

38. Missoum, K., Belgacem, M.N. & Bras, J. 2013, "Nanofibrillated Cellulose Surface Modification: A Review", Materials, vol. 6, no. 5.

39. Isogai, A., Saito, T. & Fukuzumi, H. 2011, "TEMPO-oxidized cellulose nanofibers", Nanoscale, vol. 3, pp. 71.

40. Henriksson, M., Henriksson, G., Berglund, L.A. & Lindström, T. 2007, "An environmentally friendly method for enzyme-assisted preparation of microfibrillated cellulose (MFC) nanofibers", European Polymer Journal, vol. 43, pp. 3434.

41. Ding, W.D., Chu, R.K.M., Mark, L.H., Park, C.B. & Sain, M. 2015, "Non-isothermal crystallization behaviors of poly(lactic acid)/cellulose nanofiber composites in the presence of CO2", Macromolecular Nanotechnology, vol. 71, pp. 231.

42. Khalil, H.P.S.A., Bhat, A.H. & Yusra, A.F.I. 2012, "Green composites from sustainable cellulose nanofibrils: A review", Carbohydrate Polymers, no. 87, pp. 963.

43. Diniz, J.M.B.F., Gil, M.H. & Castro, J.A.A.M. 2004, "Hornification - its origin and interpretation in wood pulps", Wood Science Technology, vol. 37, pp. 489.

44. Abdulkhani, A., Hosseinzadeh, J., Ashori, A., Dadashi, S. & Takzare, Z. 2014, "Preparation and characterization of modified cellulose nanofibers reinforced polylactic acid nanocomposite", Polymer Testing, no. 35, pp. 73.

45. Capadona, J.R., Ven Den Berg, O., Capadona, L.A., Schroeter, M., Rowan, S.J., Tyler, D.J. & Weder, C. 2007, "A versatile approach for the processing of polymer nanocomposites with self-allembled nanofibre templates.", nnano, vol. Nat Nanotechnol, no. 2, pp. 765.

46. Bulota, M., Kreitsmann, K., Hughes, M. & Paltakari, J. 2012, "Acetylated Microfibrillated Cellulose as Toughening agent in Poly (lactic acid)", Journal of Applied Polymer Science, pp. 448.

47. Jonoobi, M., Harun, J., Mathew, A.P., Hussein, M. & Oksman, K. 2010, "Preparation of cellulose nanofibers with hydrophobic surface characteristics", Cellulose, no. 17, pp. 299.

48. Oksman, K., Aitomäki, Y., Aji, M.P., Siqueira, G., Zhou, Q., Butylina, S., Tanpichai, S., Zhou, X. & Hooshmand, S. 2015, "Review of the recent developments in cellulose nanocomposite processing", Composites, no. Part A 83, pp. 2.

49. Thakur, V.K. & Thakur, M.K. 2018, Functional Biopolymers, Springer, Cham, Switzerland.

50. Zhu, Y., Romain, C. & Williams, C.K. 2016, "Sustainable polymers from renewable resources", Nature, no. 540, pp. 354.

51. NatureWorks. 2012, "NatureWorks Ingeo Polylactide: Past, Present and Future", Biopolymers & Biocomposites Workshop. Iowa State University, Minnetonka, MN, 14 Augut 2012.

52. Fukushima, K., Abbate, C., Tabuani, D., Gennari, M. & Camino, G. 2009, "Biodegradation of poly(lactic acid) and its nanocomposites", Polymer Degradation and Stability, no. 94, pp. 1646.

53. Research Institutes of Sweden AB 2015, Roadmap 2015 to 2025: Materials from nanocellulose, RISE.

54. Hubbe, M.A., Tayeb, P., Joyce, M., Tyagi, P., Kehoe, M., Dimic-Misic, K. & Pal, L. 2017, "Rheology of Nanocellulose-rich Aqueous Suspensions: A Review", bioresources.com.

55. Swain, S.K., Pattanayak, A.J. & Sahoo, A.P. 2018, "Funtional Biopolymer Composites" in Functional Biopolymers, eds. V.K. Thakur & M.K. Thakur, Springer.

56. Lee, K., Aitomäki, Y., Berglund, L.A., Oksman, K. & Bismarck, A. 2014, "On the use of nanocellulose as reinforcement in polymer matrix composites", Composites Science and Technology, , no. 105, pp. 15.

57. Murphy, C.A. & Collins, M.N. 2016, "Microcrystalline cellulose reinforced polylactic acid biocomposite filaments for 3D printing", Polymer Composites, vol. 39, no. 4, pp. 1311.

58. Tingaut, P., Zimmermann, T. & Lopez-Suevos, F. 2010, "Synthesis and Characterization of Bionanocomposites with Tunable Properties from Poly(lactic acid) and Acetylated Microfibrillated Cellulose", Biomacromolecules, vol. 11, pp. 454.

59. Scheirs, J. 2000, "Sampling an Sample Preparation" in Compositional and Failure Analysis of Polymers; A Practical Approach John Wiley & Sons, Ltd, England, pp. 30.

60. Naranjo, A., del Pilar Noriega E., Maria, Osswald, T.A., Roldan-Alxate, A. & Sierra, J.D. 2008, Plastics Testing and Characterization, Carl Hanser Verlag, Munich.